Atmos. Meas. Tech., 9, 5293–5314, 2016
www.atmos-meas-tech.net/9/5293/2016/
doi:10.5194/amt-9-5293-2016

Atmospheric Measurement Techniques
Open Access
EGU

Continuous and high-precision atmospheric concentration measurements of COS, CO_2, CO and H_2O using a quantum cascade laser spectrometer (QCLS)

Linda M. J. Kooijmans[1], **Nelly A. M. Uitslag**[1], **Mark S. Zahniser**[2], **David D. Nelson**[2], **Stephen A. Montzka**[3], **and Huilin Chen**[1,4]

[1]Centre for Isotope Research (CIO), University of Groningen, Groningen, the Netherlands
[2]Aerodyne Research Inc., MA, USA
[3]NOAA Earth System Research Laboratory, Boulder, CO, USA
[4]Cooperative Institute for Research in Environmental Sciences (CIRES), University of Colorado, Boulder, CO, USA

Correspondence to: Huilin Chen (huilin.chen@rug.nl)

Received: 12 February 2016 – Published in Atmos. Meas. Tech. Discuss.: 29 February 2016
Revised: 10 September 2016 – Accepted: 27 September 2016 – Published: 1 November 2016

Abstract. Carbonyl sulfide (COS) has been suggested as a useful tracer for gross primary production as it is taken up by plants in a similar way as CO_2. To explore and verify the application of this novel tracer, it is highly desired to develop the ability to perform continuous and high-precision in situ atmospheric measurements of COS and CO_2. In this study we have tested a quantum cascade laser spectrometer (QCLS) for its suitability to obtain accurate and high-precision measurements of COS and CO_2. The instrument is capable of simultaneously measuring COS, CO_2, CO and H_2O after including a weak CO absorption line in the extended wavelength range. An optimal background and calibration strategy was developed based on laboratory tests to ensure accurate field measurements. We have derived water vapor correction factors based on a set of laboratory experiments and found that for COS the interference associated with a water absorption line can dominate over the effect of dilution. This interference can be solved mathematically by fitting the COS spectral line separately from the H_2O spectral line. Furthermore, we improved the temperature stability of the QCLS by isolating it in an enclosed box and actively cooling its electronics with the same thermoelectric chiller used to cool the laser. The QCLS was deployed at the Lutjewad atmospheric monitoring station (60 m; 6°21′ E, 53°24′ N; 1 m a.s.l.) in the Netherlands from July 2014 to April 2015. The QCLS measurements of independent working standards while deployed in the field showed a mean difference with the assigned cylinder value within 3.3 ppt COS, 0.05 ppm for CO_2 and 1.7 ppb for CO over a period of 35 days. The different contributions to uncertainty in measurements of COS, CO_2 and CO were summarized and the overall uncertainty was determined to be 7.5 ppt for COS, 0.23 ppm for CO_2 and 3.3 ppb for CO for 1-minute data. A comparison of in situ QCLS measurements with those from concurrently filled flasks that were subsequently measured by the QCLS showed a difference of -9.7 ± 4.6 ppt for COS. Comparison of the QCLS with a cavity ring-down spectrometer showed a difference of 0.12 ± 0.77 ppm for CO_2 and -0.9 ± 3.8 ppb for CO.

1 Introduction

Carbonyl sulfide (COS) has been suggested as a potential tracer for photosynthetic CO_2 uptake (Sandoval-Soto et al., 2005; Montzka et al., 2007; Campbell et al., 2008; Berry et al., 2013; Asaf et al., 2013), as it follows the same uptake pathway into plants through stomata as CO_2 but is not generally re-emitted by plants (Protoschill-Krebs and Kesselmeier, 1992; Protoschill-Krebs et al., 1996; Stimler et al., 2010b). COS therefore provides a means to partition net ecosystem exchange into gross primary production (GPP) and respiration. As large uncertainties in the COS budget remain, field measurements of COS and CO_2 concentrations and fluxes

from leaf to ecosystem and regional scale are required for the COS tracer method to be tested and validated (Wohlfahrt et al., 2012; Berkelhammer et al., 2014). Therefore, there is a need for high-frequency and high-precision measurements techniques of COS and CO_2.

Several past studies on COS have relied on discrete (flask) samples analyzed with gas chromatographic mass spectrometry (GC-MS; Montzka et al., 2007; Stimler et al., 2010b). For example, the global atmospheric flask sampling network described by Montzka et al. (2007) has allowed a foundation for understanding COS concentrations over annual cycles on global scale. Although the GC-MS technique can be used for in situ measurements (Miller et al., 2008; Belviso et al., 2013), this technique does not typically allow for high-frequency measurements of 1 to 10 Hz. Recent developments of quantum cascade laser spectrometers (QCLSs) have enabled in situ trace gas measurements including COS. These instruments have proven to be a valuable tool for continuous high-frequency measurements of COS and CO_2 up to a frequency of 10 Hz (Stimler et al., 2010a, b; Asaf et al., 2013; Commane et al., 2013; Berkelhammer et al., 2014; Maseyk et al., 2014; Commane et al., 2015).

The required measurement precision (in this study we define precision as the standard deviation over a 2-minute period) for studies of exchange processes of COS and CO_2 between biosphere and atmosphere depend on the concentration change that these gases undergo in any given experiment. On the regional scale, COS shows seasonal variations typically between $\sim$ 100 and 150 ppt at continental sites in the Northern Hemisphere (NH) and between 40 and 70 ppt in the Southern Hemisphere and at marine sites (Montzka et al., 2007). CO_2 seasonal variations typically reach up to 15 ppm in the NH and are as low as 2 ppm at the South Pole (Zhao and Zeng, 2014). For the leaf scale, COS and CO_2 concentration changes can be substantially larger; for example, Berkelhammer et al. (2014) showed that during branch bag measurements COS generally decreased by 180 to 240 ppt during active photosynthesis and CO_2 concentrations can easily change by 200 ppm, depending on the setup. Besides the difference in requirements for precision between different experimental setups, the type of analyses intended for a dataset also determines the requirements for precision and accuracy of the measurements. If the intention is to compare atmospheric concentrations across sites, then accuracy is important because data from different sites must be on consistent scales. In contrast, short-term precision is more important than accuracy when differences between heights are to be interpreted (e.g., as in estimation of fluxes from profile measurements). Following the K-parameterization formulation of the flux-gradient method (e.g., Meredith et al., 2014), $F = -K\Delta C/\Delta z\rho$, the precision required to capture the concentration differences between heights (ΔC) mostly depends on the size of the fluxes F, the height difference Δz, the turbulence conditions, which are represented by the eddy diffusivity K, and to a lesser extent on the molar density of air ρ. To be able to capture COS fluxes of, for example, 10 pmol m^{-2} s^{-1} over a height difference of 20 meters, the measurement precision of COS should be better than 0.5 ppt under high turbulent conditions ($K = 10\,m^2\,s^{-1}$) and 4.8 ppt under low turbulent conditions ($K = 1\,m^2\,s^{-1}$). If we were to infer the gross fluxes from chamber measurements with ΔCO_2 (the difference between in- and outgoing chamber concentrations) measurable from 1 ppm, then, given the leaf-scale relative uptake (LRU) ratio of COS / CO_2 1.5–4.0 (Stimler et al., 2010b; Seibt et al., 2010; Berkelhammer et al., 2014), our goal would be to have measurement precisions of COS better than 1.9–5.0 ppt for COS (calculated from LRU and scaling with ΔCO_2 and the ratio of COS/CO_2 mole fractions gives, for example, $1.5 \times 1 \times (500/400) = 1.9$ ppt at the ambient level of 500 ppt and 400 ppm CO_2).

Measurement instruments for long-term atmospheric trace gas concentration monitoring need to meet different requirements than, for example, eddy-covariance measurements. The eddy-covariance technique requires high-frequency data (> 10 Hz), which typically adversely affect the precision of the measurements compared to 1 Hz data, and requires an averaging period of about 10 to 30 min. In contrast to the high frequency required for eddy-covariance measurements, lower-frequency measurements (1 Hz) provide useful results over extended measurement periods and enhance the precision of any individual measurement. Furthermore, measurements for long-term monitoring do not require fast response, and thus it is not necessary to operate the instrument at high flow rates. As a matter of fact, low flow rates are preferred so that working standards can be used over a long period. This reduces the additional logistics needed for calibration gases, such as filling, calibration and transportation of the standards (Xiang et al., 2014). Besides in situ measurements, flask or canister measurements can be a valuable tool for providing information about ambient concentrations of COS as well. For example, flask measurements were used before when constructing an historical record from firn air (Montzka et al., 2004), during field campaigns (White et al., 2010; Blonquist et al., 2011) and for long-term monitoring (Montzka et al., 2007). In this research we developed a robust setup for high-precision and long-term monitoring of ambient concentrations of COS, CO_2, CO and H_2O at different heights from the Lutjewad monitoring station in Groningen, the Netherlands. To this end we employed a "QCL Mini Monitor" from Aerodyne Research Inc. (Billerica, MA, USA) that can operate autonomously and requires little operator attention. We designed an optimal strategy for "zero" air spectral correction and calibration for accurate measurements and we assessed the correction for water vapor interference. In this paper we aim to evaluate and improve the performance of the instrument. We will show the precision and accuracy of the instrument with over half a year of field data and measurements of working standards, and we compare the measurements with other instrumentation. Furthermore, we evaluate the total uncertainty of the measurements by combining the

uncertainties of scale transfer, water vapor corrections and the measurement precision. Based on the precision and accuracy that we derive from these experiments, we discuss the suitability of COS measurements on this instrument for different purposes, that is, for interpreting profile measurements and comparing concentrations across sites. In addition to the experimental setup for continuous in situ measurements we developed a setup to analyze flasks, which we used to make a comparison with GC-MS measurements of flasks and to assess the laboratory-derived correction for water vapor interference.

2 Experimental setup

Before the actual deployment of the instrument in the field, we performed laboratory tests to assess the accuracy and traceability of the QCLS measurements and to develop procedures for applying corrections as needed. Here we describe the laboratory tests and we give detailed information about the instrumentation and field setup.

2.1 Instrumentation

The QCL Mini Monitor that we use is a tunable diode laser absorption spectrometer (TILDAS) using a single continuous-wave quantum cascade laser (Alpes Lasers), which is cooled with a Peltier element to −19.8 °C, and using a single photodiode infrared detector (Teledyne Judson Technologies; McManus et al., 2010). The waste heat from both the laser and detector is removed with a recirculating mixture of water containing 25 % ethanol, which is temperature controlled with a thermoelectric chiller, ThermoCube 300 (Solid State Cooling Systems, USA). The instrument was initially set to simultaneously measure COS, CO_2 and H_2O at wavenumbers 2050.397, 2050.566 and 2050.638 cm^{-1}, respectively. We extended the range of the laser current to include measurements of CO at 2050.854 cm^{-1}. Figure 1 shows the simulated transmission spectrum of ambient concentrations of COS, CO_2, CO and H_2O as obtained through the HITRAN 2012 database (Rothman et al., 2013). The precision and accuracy of the measurements will be discussed in Sect. 3.1.

The instrument consists of a 0.5 L astigmatic Herriott style multi-pass absorption cell (McManus et al., 2010) with an effective path length of 76 m. The cell has a temperature between 20 and 24 °C, depending on the room temperature and the temperature setting of the thermoelectric chiller. The cell is kept at a constant pressure of 53.3 hPa (40 Torr) with an inlet valve that is controlled by the TDLWINTEL program (Aerodyne Research Inc., Billerica, MA, USA) based on the measured cell pressure. The same software manages the data acquisition and spectral analysis (Nelson et al., 2004) and calculates dry air mole fractions in real time (1 Hz) through nonlinear least square spectral fits combined with the measured cell temperature and pressure, a constant path length

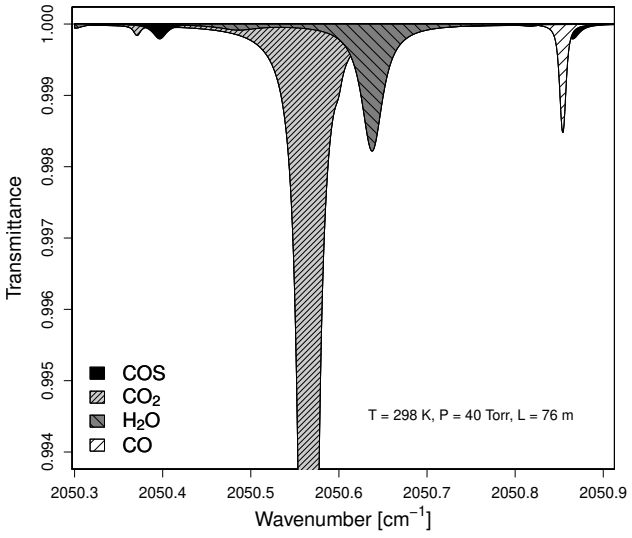

Figure 1. Simulated transmission spectrum of ambient concentrations of COS (500 ppt), CO_2 (500 ppm), H_2O (1.5 %) and CO (200 ppb) with sample cell conditions: temperature 298 K, pressure 53.3 hPa (40 Torr) and the absorption path length 76 m. A small water band at 2050.5 cm^{-1} can interfere with COS at 2050.4 cm^{-1} and can affect the COS correction for water vapor without a split fit at 2050.45 cm^{-1} (Sect. 2.3).

and the HITRAN 2012 database cross sections as a function of wavelength. The spectral fit for CO is separated from the fit for COS, CO_2 and H_2O as there is slight interaction of the CO peak with a second absorption line of COS. The COS fit close to the CO peak is linked to the COS peak at lower wavenumbers to improve the fitting for CO. This is achieved by fitting the spectra in two steps: first the mole fractions are determined for both COS peaks independently; second the CO concentration is recalculated with the fixed COS concentration derived from the separated COS peak in the first step.

The TDLWINTEL software has the option to store raw spectra. These spectra can later be used for re-analysis using the so-called "playback" mode of the software. The spectral parameters (line shape and position) for the fits are taken from the HITRAN database (Rothman et al., 2013). The sample spectra are normalized with a "zero" air spectrum to remove background spectral structures and to remove absorbance external to the multi-pass cell (Stimler et al., 2010a; Santoni et al., 2012). The "zero" air spectrum is periodically determined when the cell is flushed with high-purity nitrogen (99.99999 %), which we will now refer to as "background" measurement. The nitrogen is first passed over a gas purifier (Gatekeeper, CE-500K-I-4R) to remove CO that is often found in such nitrogen cylinders. The frequency of the laser is locked based on the spectrum measurement of the high strength CO_2 line at 2050.566 as shown in Fig. 1. For automatic start-up, a gas sealed in an aluminum reference cell can be flipped into the optical beam. The reference cell was

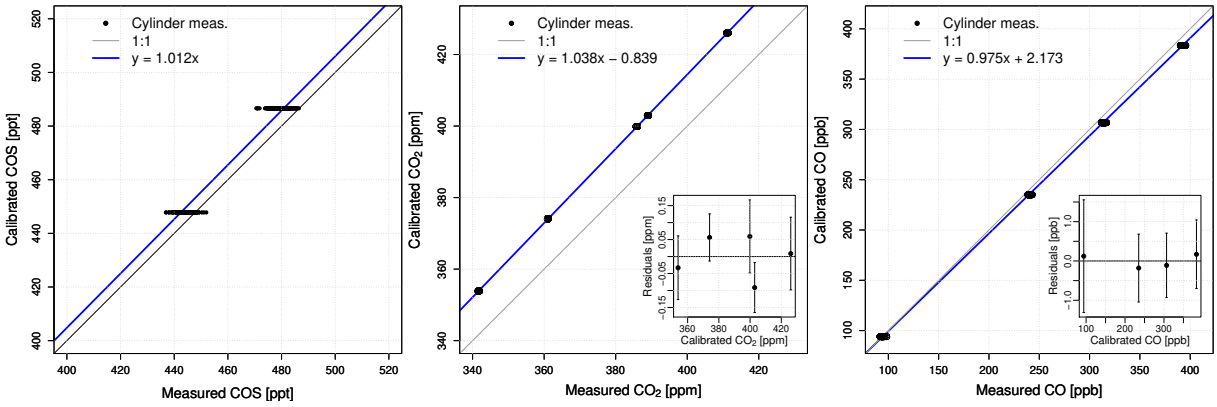

Figure 2. Response curves determined with NOAA/ESRL calibration standards, including the residuals of the fit. The NOAA/ESRL calibration standards are calibrated on NOAA-2004 COS scale, WMO-X2007 CO_2 scale (Zhao et al., 2006) and WMO-2004 CO scale (Novelli et al., 2003). Each standard was measured for 5 min. The measured mole fractions shown on the x axes are mole fractions calculated through the TDLWINTEL software but are corrected for drift using a reference standard. The drift was on the order of 8 ppt for COS, 3 ppm for CO_2 and 5 ppb for CO and would have given biased results if this were not corrected for.

filled with 8 hPa (6 Torr) COS and 27 hPa (20 Torr) CO. Initially, we could use the peak position of COS in the reference cell to determine the frequency of the laser. However, COS did not last longer than a few months in the reference cell so thereafter the laser frequency was locked only based on the peak position of CO, which did not impact the results.

2.2 Calibration strategy

To allow comparison of QCLS measurements with other instrumentation and across different sites requires traceability to a primary scale. Laboratory tests were conducted to characterize the response of the instrument against ambient air standards from NOAA/ESRL, which were subsequently used to transfer the calibration scale to working standards. Moreover, we performed tests to understand the frequency required for background and reference measurements to ensure reliable and accurate results.

2.2.1 Instrument response

To characterize the response of the instrument for COS, CO_2 and CO mole fractions we used six aluminum cylinders that were calibrated at the NOAA Boulder laboratories on NOAA-2004 COS scale, WMO-X2007 CO_2 scale (Zhao et al., 2006) and WMO-X2004 CO scale (Novelli et al., 2003). Five of the six standards were calibrated for CO_2, four for CO and two for COS. The internal surfaces of the COS calibrated cylinders were Aculife treated. Figure 2 shows that the response curves are linear for CO_2 (between 354 and 426 ppm) and CO (between 94 and 384 ppb). Furthermore, the residuals of these curves do not show signs of nonlinearity. For COS, conclusions about the linearity of the response are not possible given that we had only two calibrated standards. As the response is linear for CO_2 and CO, we assume that the response is linear for COS as well. The NOAA/ESRL calibrated standards cover a wide range of CO_2 and CO concentrations and response curves that were determined for these gases were consistent when the experiment was repeated. The factor 1.038 to transfer the QCLS CO_2 measurements to the WMO scale is slightly different from the factor 1.05 found by Commane et al. (2013). For COS the concentration range of the NOAA/ESRL calibration standards was smaller, between 447.8 and 486.6 ppt, and combined with the lower precision of these measurements, the response curve has large uncertainty. Therefore, repeating the experiment resulted in varying response curves, with an average slope equal to 0.99 and the minimum and maximum slope equal to 0.87 and 1.04 respectively. The response curve shown in Fig. 2 is the curve where the two NOAA/ESRL calibration standards measurements showed the lowest standard deviations: 2.7 and 3.0 ppt, with the average standard deviation over different experiments equal to 4.4 ppt. In the next section we will discuss different calibration methods to deal with the higher uncertainty of the COS response curve. Furthermore, we tested the stability of the response of COS, CO_2 and CO with hourly measurements of three working standards over a period of 35 days during field measurements. The results of this will be shown in Sect. 3.1.

2.2.2 Working standards

In this study we use working standards to represent high-pressure cylinders that are calibrated against NOAA or WMO standards in our laboratory. The working standards are used for two purposes: (1) to correct for instrument drift during field measurements and link the measurements to the NOAA or WMO scales (in this case we refer to these standards as reference standards) and (2) to assess the accuracy of the measurements (in this case we refer to these standards

Table 1. CO_2 and CO calibration values together with 1σ uncertainties of the calibration curves as obtained with the QCLS and a cavity ring-down spectrometer (CRDS) for comparison of calibration results. COS calibration values could not be compared with that from other instrumentation.

	CO_2 (ppm)		CO (ppb)	
	QCLS	CRDS	QCLS	CRDS
Cyl. no. 1	412.33 ± 0.12	412.43 ± 0.08	97.8 ± 1.7	97.6 ± 3.0
Cyl. no. 2	398.30 ± 0.12	398.13 ± 0.08	119.1 ± 1.7	119.1 ± 3.0

Table 2. COS calibration values for our real-air working standards as obtained from three different calibration approaches: (1) with response from the two NOAA/ESRL calibration standards and a zero point, (2) with the two NOAA/ESRL calibration standards and the curve not forced through a zero point and (3) using a single bias correction. The NOAA/ESRL calibration standards have COS concentrations 447.8 and 486.6 ppt. The calibration measurement was repeated three times; results are shown as the average over the three measurements and uncertainties indicate the standard deviation over the three measurements.

	Cyl. A	Cyl. B	Cyl. C	Cyl. D
1. Through NOAA/ESRL standards and 0	393.0 ± 2.2	448.8 ± 4.7	473.6 ± 1.5	504.1 ± 0.7
2. Through NOAA/ESRL standards and not 0	379.2 ± 8.3	445.5 ± 4.4	474.7 ± 1.9	510.8 ± 4.7
3. Single bias correction	390.9 ± 2.6	445.8 ± 3.9	476.6 ± 2.4	506.6 ± 2.1

as target standards). The working standards used in this study are aluminum gas cylinders (Luxfer, max. 200 bar) filled to high pressure with ambient air at the Center for Isotope Research of the University of Groningen using an oil-free air compressor (RIX SA-3) and are used in combination with two-stage regulators (Scott Specialty Gases, model 14). The working standards differ from the NOAA/ESRL calibration standards in the sense that they are uncoated. To trace the working standards that we used in the field we refer to these with numbers 1, 2 and 3 throughout the paper. Other working standards that were used in this paper but not in the field are referred to as "A","B", "C" and "D". Using the linear regression curve that we found in Fig. 2, we determined mole fractions in these working standards by considering response curves derived from measurements of the NOAA/ESRL calibration standards. Results of calibrations of three working standards with the QCLS are shown in Table 1 for CO_2 and CO. We calibrated the same working standards with a cavity ring-down spectrometer (CRDS; Picarro Inc. model G2401-m) using the same standards linked to the WMO scale. Calibrations with the QCLS for CO_2 and CO agree with calibrations from the CRDS within their uncertainties, which gives confidence in our calibration method. For COS we could not compare our calibrations with that from other instrumentation.

As we saw in Sect. 2.2.1, the response curve of COS is difficult to determine due to the lower instrument precision and the narrow COS concentration range of the NOAA/ESRL calibration standards. These factors introduce uncertainty in assigning values to the working standards that will be used on-site, especially for those having COS mole fractions outside of this range. Besides that, the number of available calibrated standards used to transfer the scales to other cylinders may be limited in labs, especially for COS, as this gas is usually not one of the standard measured species. The question is therefore what method is suitable to transfer the scale to the working standards for COS. To test this, we re-analyzed calibration measurements in different ways: (1) with response from the two NOAA/ESRL calibration standards and the curve forced through a zero point, (2) with two NOAA/ESRL calibration standards and the curve not forced through zero and (3) with a single bias correction using a NOAA/ESRL calibration standard that has the concentration closest to the working standard.

Table 2 shows the assigned values on the working standards considering the different approaches. The calibration measurement was repeated three times and results are here shown as the average over the three measurement. The fact that the cylinder values need to be extrapolated causes larger deviations compared to when the curve is forced through a zero point (see, e.g., cylinder "A" in Table 2). Therefore, when working standards have concentrations outside the range covered by the NOAA/ESRL calibration standards, method 1 is preferred because it avoids extrapolation of the calibration curve by using the zero point. However, as we saw in Sect. 2.2.1 it is difficult to accurately determine a calibration curve due to the lower precision of the measurements and the narrow COS concentration range of the NOAA/ESRL calibration standards, which holds for both methods 1 and 2. In this study we therefore calibrate cylinders and field measurements under the assumption that the data follow a calibration curve with a slope equal to 1 (in Sect. 2.2.1 we saw that the average slope of different calibration experiments was equal to 0.99) and we apply a single bias correction, which is applied in Table 2 as method 3. Theoretically, methods 1 and 2 would give the results closest to

Table 3. Standard deviation (SD) over minute-averaged data of COS, CO_2 and CO over the 19 h measurement period for different correction frequencies using reference measurements.

	Uncorrected	1 h corr.	30 min corr.	15 min corr.
COS SD (ppt)	11.8	9.6	5.3	4.6
CO_2 SD (ppm)	0.26	0.12	0.09	0.08
CO SD (ppb)	0.8	0.7	0.3	0.3

reality, but here we observe that the difference of method 3 against methods 1 and 2 is small (on average 1.3 ppt) and the result is often in between those of methods 1 and 2. We therefore consider the single bias correction as a good compromise when a calibration curve cannot accurately be determined.

2.2.3 Background and reference strategy

Background measurements with dry nitrogen are required to reduce the effect of curvature of the baseline spectra and are typically done every 2, 5 or 30 min by other users of similar QCLS analyzers (Stimler et al., 2010a; Commane et al., 2013). When we tested the required frequency of background measurements we found that COS concentrations can shift to another level, either up or down, uncorrelated with instrument parameters such as temperature, and even when the background measurements were done shortly after each other (every 10 min). In a test where we measured cylinder air over a period of 5 h, alternating with background measurements every 10 min, we found that on average the COS concentration shifts by 5 ppt after every background measurement, but in 32 % of the cases the shift is larger than 10 ppt, with peaks up to 37 ppt. We could not correlate these shifts to changes in instrument temperature or inlet pressure or to the length of the background measurement itself. As we could not find correlations with any parameter, the reason for these shifting concentrations after background measurements is unknown. To be able to correct for the concentration shifts for accurate concentration measurements requires measurements of reference gases at least once within every background cycle. Therefore, increasing the background frequency automatically leads to greater use of a reference cylinder gas. As we also need to consider cylinder logistics (filling, calibrating and transportation), we decided to do less frequent background measurements (once every 6 h) with reference cylinder measurements in between. Lowering the background frequency to 6 h did not negatively affect the measurement precision, but the accuracy of the measurements is affected due to instrument drift over the period in between the background measurements. The frequency of reference cylinder measurements that is needed to correct for the instrument drift depends on the rate with which the instrument temperature changes. Hourly measurements of reference standards in the field (during a later field campaign in Hyytiälä, Finland, not shown here) showed that concentrations drift on the order of 100 ppt (COS), 2 ppm (CO_2) and 10 ppb (CO) per degree change of the electronics temperature in a few hours when the instrument was placed in an enclosed box and when the electronics section was actively cooled (see Sect. 2.5). To test the frequency of reference measurements that is needed to remove drift due to temperature changes, we measured cylinder air over a period of 19 h, alternating with a reference gas every 15 min. During this measurement period the electronics temperature changed by 0.1 °C due to changes of the room temperature, where the most rapid change was 0.06 °C in 30 min. Without correcting the data, the standard deviation of the minute-averaged data is 11.8 ppt for COS, with drift up to 40 ppt. Correcting the data with reference measurements from every 15 min lowers the standard deviation to 4.6 ppt, while correcting only every 30 and 60 min gives a standard deviation of 5.3 and 9.6 ppt respectively. See Table 3 for an overview of the standard deviations of COS, CO_2 and CO. Based on these results we can say that reference measurements every 30 min are sufficient to remove drift within 5.3 ppt with temperature changes up to at least 0.06 °C per 30 min. Field measurements have shown that with corrections from 30 min reference measurements, drift is still sufficiently removed with temperature changes up to 0.2 °C per 30 min. Furthermore, improving the temperature stability of the instrument could reduce the drift such that reference measurements are needed less frequently. The effect of improved temperature stability was tested during field operation of the QCLS at the Lutjewad station (see Sect. 2.5).

2.3 Water vapor interference correction

The concentration measurements of gases determined through light absorption spectrometry can be affected by water vapor in the sample air in two ways: (1) by spectroscopic effects (enhanced pressure broadening or direct spectral interference), which will directly modify the absorption spectrum, and (2) through dilution of the sample air, which linearly depends on water vapor concentrations. The water vapor interference can be prevented by drying the air before measurement. However, this requires adding a drier to the sampling inlet lines and, depending on the drier, it can require additional maintenance, which is not favorable for unattended autonomous measurements. As the QCLS includes measurements of H_2O, water vapor interferences can be accurately accounted for in the calculation of dry air mole fractions of the other gases. We determined the water va-

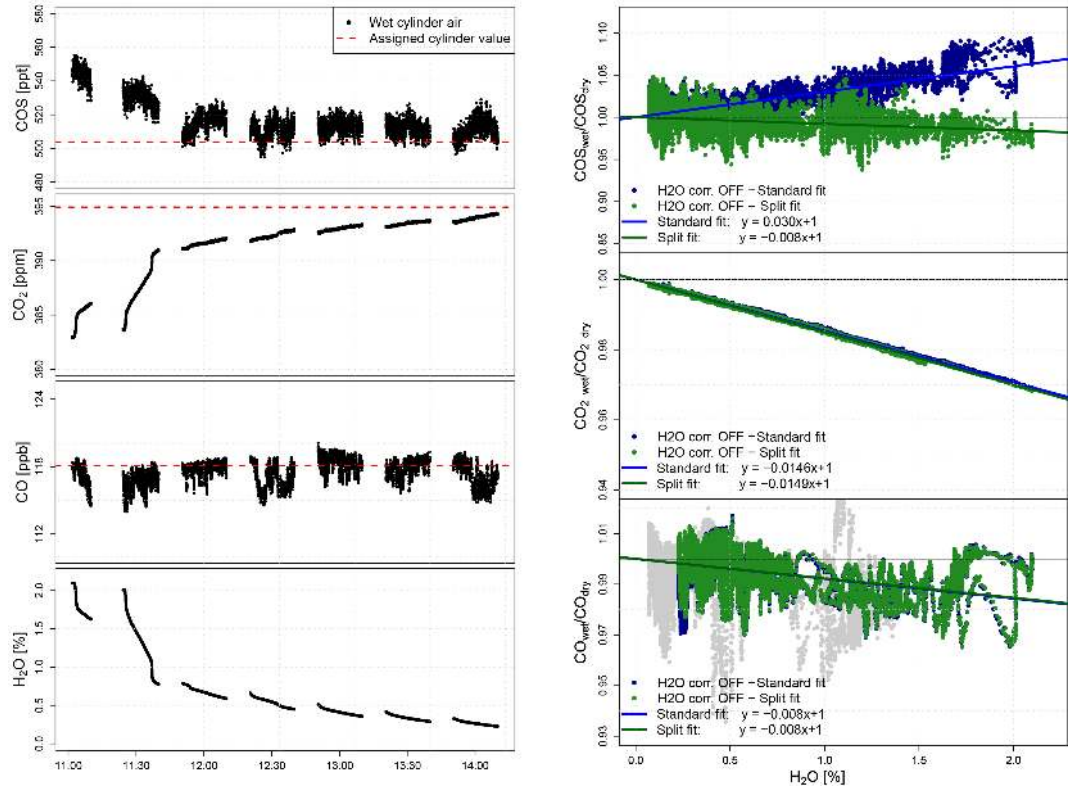

Figure 3. Left: water vapor experiment where cylinder air was humidified with wet silica gel and no water vapor correction was applied to the data. Right: wet over dry ratio of COS, CO_2 and CO vs. H_2O as obtained from multiple water vapor experiments with humidified cylinder air. The data show the linear dependence with H_2O when the TDLWINTEL water vapor correction was turned off with the standard fit (blue) and with the split fit (green).

por dependence of mole fractions reported by the instrument (TDLWINTEL software) for COS, CO_2 and CO from laboratory experiments. To do this we measured dry and humidified cylinder air alternately. We humidified the cylinder air with wet silica gel in a filter, giving a water vapor profile from 2.1 % down to 0.2 % H_2O in the sample air when the line was flushed (Rella et al., 2013). The interaction of silica gel with COS, CO_2 and CO was tested by drying the air with magnesium perchlorate or a cryogenic system after the air had passed the wet silica gel. No interaction with COS, CO_2 and CO was found for silica gel, magnesium perchlorate and the cryogenic system: the average difference between the unaffected and humidified/dried silica gel air was maximum 1.0 ± 1.9 ppt for COS, 0.11 ± 0.13 ppm for CO_2 and 0.3 ± 0.4 ppb for CO. Furthermore, we found that a 0.3 nm molecular sieve, which is commonly used to remove water vapor, removes all COS from cylinder air. The dry air cylinder measurements were used as a reference during the experiment to account for instrumental drift. Figure 3 (left) shows the mole fractions of the humidified air measurements during the experiment with the TDLWINTEL water vapor correction turned off. The right plots in Fig. 3 show how the wet / dry ratios of the COS, CO_2 and CO concentrations relate to H_2O when the TDLWINTEL water correction was turned off (blue). For this figure we combined three water vapor tests, of which one of the three was done with the TDLWINTEL water correction turned off and the other two had the TDLWINTEL water correction turned on. We ran the playback mode of the TDLWINTEL software to get the data of these water vapor experiments for the case that the correction was turned off, when the real time data were obtained with the correction on. For CO only two of the three experiments are used in the analysis because the third showed larger scatter (colored in gray), indicating instability of the QCLS. We will further discuss the precision of the measurements and its variation over time in Sect. 3.1. The linear regression is derived from averages over every 0.1 % H_2O range such that the regression is not influenced by the fact that there are more data points towards lower H_2O concentrations. Figure 3 shows that the COS, CO_2 and CO wet / dry ratios are all linearly dependent on H_2O. When wet air mole fractions are measured (that is, the TDLWINTEL water vapor correction is turned off), these curves could act as a water vapor correction factor to obtain dry air mole fractions. The effect of H_2O on the species is +3.0 % for COS, −1.46 % for CO_2 and −0.8 % for CO per % H_2O. The standard de-

viation of the residuals of the fit translates to an uncertainty in concentrations of 2.9 ppt for COS (at a concentration of 450 ppt), 0.10 ppm for CO_2 (at 400 ppm) and 1.1 ppb for CO (at 150 ppb). These uncertainties are dependent on the COS, CO_2 and CO concentrations. The fact that CO_2 and CO show an inverse correlation with H_2O indicates that these species are primarily affected by the dilution effect of water vapor. To the contrary, COS shows a positive relation with H_2O. The reason for this positive correlation is that the baseline shape of the spectra is distorted by a small H_2O peak on the left of the larger H_2O peak to the right of the large CO_2 peak (see Fig. 1). A potential solution to this would be to split the fit between the COS peak and the small H_2O peak, which we will now refer to as "split fit" (in contrast to the "standard fit"). In Fig. 3 (right) the results with the split fit are shown in green. For CO_2 and CO the green curve does not differ significantly from the blue curve, as would be expected. For COS the correlation with H_2O is now negative, with an effect of -0.8 % per % H_2O. A slope of -1 % would be expected due only to pure dilution; however, pressure broadening by water vapor affects the mole fractions as well. Within TDLWINTEL the width of the peaks is fixed based on the line shape information from the HITRAN database, which is only for air broadening with N_2 and O_2. Water broadening can be greater than air broadening. To correct for the pressure broadening effect the software modifies the width of the absorption line through the so-called air "broadening coefficients", which are specific for every spectral line of a certain species. The later version of TDLWINTEL can also use the water broadening effect by increasing the air broadening coefficients from HITRAN. The residual error of the fit, which is caused by the broadened absorption line but not properly adjusted line width, affects the mole fraction and thereby the slope of the curves in Fig. 3. This can explain why the slopes differ for the different species. Besides that, the measured H_2O concentration has an uncertainty, which contributes to the deviation of the slope from -1 %.

Using the playback mode we tried to find the most optimal water broadening coefficients to sufficiently correct for water vapor using TDLWINTEL. We did this for the three different water vapor tests and for both the standard fit and the split fit. For the standard fit we could not find optimized broadening coefficients for COS because turning the TDLWINTEL correction on caused an opposite correction and resulted in larger deviations from the assigned cylinder value due to the effect of the H_2O peak on the baseline. For the standard fit, the optimized broadening coefficients varied between 2.1 and 2.2 for CO_2 and between 1.0 and 2.0 for CO for the different experiments. For the split fit we did find optimized coefficients for COS between 1.0 and 1.4 for the different experiments; for CO_2 and CO the same results were found as for the standard fit. When the different experiments were combined, the optimized broadening coefficients are equal to 1.0, 2.15 and 1.0 for COS, CO_2 and CO respectively, where the values for CO_2 and CO can be used for both the standard and split fit, and the value for COS is only suitable for the split fit. As the optimization of the broadening coefficients depends on the curves in Fig. 3 (most optimal is when the slopes are equal to zero), the uncertainty of the water correction also entails an uncertainty in the broadening coefficients. We find that the uncertainties of the broadening coefficients are equal to 0.5 (COS), 0.03 (CO_2) and 0.7 (CO). This means that varying the broadening coefficient of COS from 1.0 to 1.5 only changes the COS concentration by 2.9 ppt (at a concentration of 450 ppt COS). The large uncertainties of the COS and CO broadening coefficients therefore indicate that these coefficients have relatively little effect on the concentrations.

Table 4. Different water vapor correction strategies based on the software fitting parameters (standard or split fit) and with the TDLWINTEL correction turned on or off. When the TDLWINTEL correction is turned on the values indicate the broadening coefficient used for the different species, and when it is turned off the values indicate the slope of the correction curve as determined in Fig. 3 with $y = \text{slope} \times H_2O + 1$ with H_2O in percent and y the wet / dry ratio of the gas.

	TDLWINTEL	Broadening coefficient or slope		
	correction on/off	COS	CO_2	CO
Standard fit	on	–*	2.15	1.0
	off	0.030	−0.0146	−0.008
Split fit	on	1.0	2.15	1.0
	off	−0.008	−0.0149	−0.008

* No broadening coefficient could be derived; however, we found that for a broadening coefficient of 1.5 with the standard fit the slope of the curve for COS is equal to 0.031, which can be applied as an extra correction on top of the TDLWINTEL correction.

Different water vapor correction strategies can now be considered and are summarized in Table 4. An appropriate direct water correction for COS is not possible with the combination of the standard fit and the TDLWINTEL correction on. However, a correction curve can still be applied to these data with a curve that is determined with the same broadening coefficients as are used for the original data to be corrected. Here we found that for a broadening coefficient of 1.5 with the standard fit the slope of the curve for COS is equal to 0.031. We continued to test the performance of the water vapor correction based on the standard fit and the TDLWINTEL correction off. We applied the correction curves to field measurements over a period of 35 days in March and April 2015. In Sect. 3.2 we will compare the dry air mole fractions with measurements of a collocated CRDS for CO_2, CO and H_2O and with dry air flask sample measurements for COS.

2.4 Flow schematics for measurements at the Lutjewad station

In July 2014 we deployed the QCLS in the field for measurements at the Lutjewad monitoring station in the Netherlands (60 m; 6°21′ E, 53°24′ N; 1 m a.s.l). We use three diaphragm pumps (KNF N-86) to keep the inlet lines well flushed be-

tween the inlet at the tower and the laboratory where the analyzer is positioned (up to 60 m length in the tower and 30 m from the tower to the lab building) with a flow of 2 L min^{-1}. Just in front of the pumps we split the line with a tee junction to get a subsample from the tower lines. These subsamples are pulled through the sample cell with an oil-free dry scroll pump (Varian TriScroll) downstream of the cell of the QCLS. Half-inch Synflex (Decabon) tubing is used in the tower and in front of the KNF pumps. We have tested the interaction of Teflon and Synflex with COS: no significant differences in COS mole fractions were found when the air flow was alternately passed over stainless steel and Teflon (0.9 ± 1.9 ppt) or Synflex (0.7 ± 2.6 ppt). We did observe COS production from the KNF N-86 pumps, but this did not cause problems for the measurement sampling as these pumps were placed on the bypass lines. We use a 5.0 µm Teflon filter at the inlet of the tower sample lines to prevent dust, sand and salt coming into the lines. In front of the analyzer we use another 0.5 µm stainless steel filter (Swagelok) to prevent pollution of the sample cell. A check valve is placed between the analyzer and the vacuum pump to prevent unfiltered room air to enter the cell through the pump in case the vacuum pump suddenly stops. A needle valve was placed between the cell and the vacuum pump to control the flow of the system at 0.16 L min^{-1}, resulting in a 90 % response time of ~ 15 s. We use a multi-position Valco valve (VICI; Valco Instruments Co. Inc.) to switch between sample lines from different heights in the measurement tower and to working standards. The Valco valve is controlled by the TDLWINTEL software in which one can set the sequence and duration of the valve ports to be measured. An interval is set for automatic hourly repetition of the sequence. Until January 2015 we used a solenoid valve (Parker) to switch between dry nitrogen and cylinder or ambient air. However, we found that this solenoid valve was leaking and was thereby diluting the cylinder and ambient air measurements with dry nitrogen. On 7 January 2015 we changed the setup such that the Valco valve also controlled switching to the dry nitrogen. The Valco valve, KNF pumps, air purifier and 0.5 µm filter are built into a 19 in. rack with 1/8 in. stainless steel tubing.

For our setup, every hour starts with a measurement from a reference and target standard (3 min each). Subsequently, the system alternates between three measurement heights where every height is measured for 8 min, meaning that every height is measured twice an hour. The reference standard was measured every half hour to remove instrument drift. In March 2015 we measured an extra reference gas once every hour, which was used to test the stability of the instrument response over a period of 35 days (the results will be shown in Sect. 3.1). Background measurements were done every 6 h with dry nitrogen over 60 s. Before the actual background measurement is done, the cell is first flushed for 2.5 min to make sure that water vapor is removed from the cell by 99 %.

2.5 Temperature stability

We noticed that under lab conditions, when the temperature is controlled within ~ 0.2 °C, the precision of the instrument was typically better than with the highly changing temperatures up to 2 °C at the measurement station during the course of the day. These temperature dependencies were also observed with other QCLS analyzers in Xiang et al. (2014) and Berkelhammer et al. (2014). Before we made any modifications, the electronics temperature (T_{electr}) varied with 0.91 °C with every degree of changing room temperature (T_{room}) and the cell temperature (T_{cell}) varied with 0.11 °C °C^{-1}. Xiang et al. (2014) showed the potential to improve the temperature stability with an active temperature control using an Oasis 3 chiller (Solid State Cooling Systems, USA) of which the set point can be controlled with the TDLWINTEL software. They improved the T_{cell} variability of 0.03 °C °C^{-1} without active temperature control to 0.0005 °C °C^{-1} with active control. We improved the temperature stability of the instrument with only the ThermoCube chiller, for which we extended the cooling loop to a heat exchanger attached to the fan of the electronics section. This way, the air going into the electronics section for ventilation is actively cooled. Moreover, we have put the analyzer in an enclosed box to add an extra layer of temperature isolation. With these modifications the temperature variability of T_{electr} improved to 0.21 °C °C^{-1} and to 0.07 °C °C^{-1} for T_{cell}.

2.6 Measurements of COS from flasks

Besides testing the QCLS for continuous in situ measurements, we explore the suitability of the QCLS for measuring air from flasks. We developed a means to analyze flasks; this allowed a comparison between the QCLS and GC-MS measurements from the NOAA Boulder laboratory (Montzka et al., 2007). For this analysis we filled flasks from cylinders, such that, besides the instrument comparison, we were able to assess the accuracy of the flask measurements and check the methodology for assigning values to our working standards based on the NOAA/ESRL calibration standards. Four pairs of glass flasks with a volume of 2.5 L were filled to 2.5 bar with dry air from two of our working standards and the two NOAA/ESRL calibration standards. The working standards were calibrated for COS by comparing their response on the QCLS to the NOAA/ESRL calibration standards as described in Sect. 2.2.2. The four cylinders contained COS concentrations between 447.8 and 486.6 ppt. The flask measurement setup using the QCLS is similar to that of routine tower measurements but with a few modifications. A pressure sensor was added to monitor the pressure in the flasks. Furthermore, a diaphragm pump with a shut-off valve was used to remove residual air from previous flask measurements in the connecting tube and to test the lines for leaks. In Fig. 4 the placement of the pressure sensor and diaphragm pump is indicated; they are separated from the field mea-

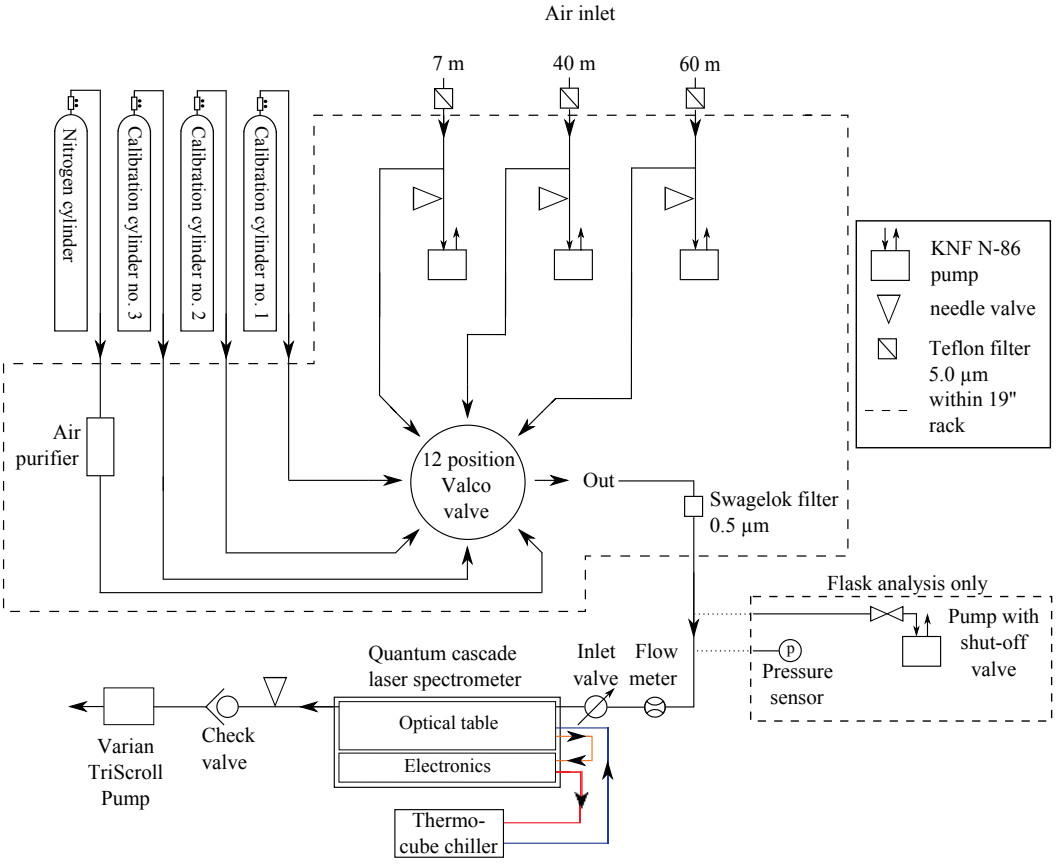

Figure 4. Schematic overview of the instrument setup for tower profile measurements at the Lutjewad monitoring station. The pressure sensor and pump with shut-off valve were added for flask measurements only (see Sect. 2.6).

surement setup as it is used for flask measurements only. Air from reference and target tanks was introduced before measuring the actual flask sample to calibrate the measurements to the NOAA scale. We did not use measurements of a reference gas after the flask measurement as the stability of the measurements is affected by the larger pressure difference between the flask and the reference cylinder. Two measurements of 2 min each were done on each flask and the results were averaged to derive the final value. The results of these flask measurements will be shown in Sect. 3.2.

We also measured dry air flask samples to test if the water vapor correction that we determined in Sect. 2.3 sufficiently removes the effect of water vapor on calculated mole fractions. To that aim, flasks were filled to ambient pressure as part of a standard flask sampling routine at the Lutjewad station (Neubert et al., 2004). The air samples are dried with a cryogenic system prior to collecting. The flasks were stored for maximum 1.5 months before being measured. The same measurement strategy as for the NOAA/ESRL comparison was used, and for these flasks two measurements of ~ 1.5 min could be done before an inlet pressure of 0.3 bar was reached. We did not observe any dependence of measured dry air mole fractions in air from the flasks with the inlet pressure below ambient. The measurement results will be shown and compared with the in situ QCLS measurements in Sect. 3.2.

3 Results and discussion

3.1 Precision and accuracy

We assessed the measurement uncertainty and accuracy with the hourly measurements of the reference and the target gases over the period from August 2014 until April 2015. As mentioned previously, each reference and target gas was measured for 2 min. The mean value of the hourly instrument-reported and uncorrected 2-minute measurements are shown in Fig. 5. In Fig. 6 the standard deviation of these measurements is shown. Figure 5 also includes the electronics temperature of the QCLS. The cylinder measurements show that concentrations can drift substantially; i.e., COS concentrations easily vary by 50 to 100 ppt. However, on the long term, concentration changes are not correlated with temperature, which changed by 13 K throughout the year. The concentration shift on 7 January 2015 (especially visible in CO_2) happened after eliminating the leaking solenoid valve that caused mixing of nitrogen into the tubing that deliv-

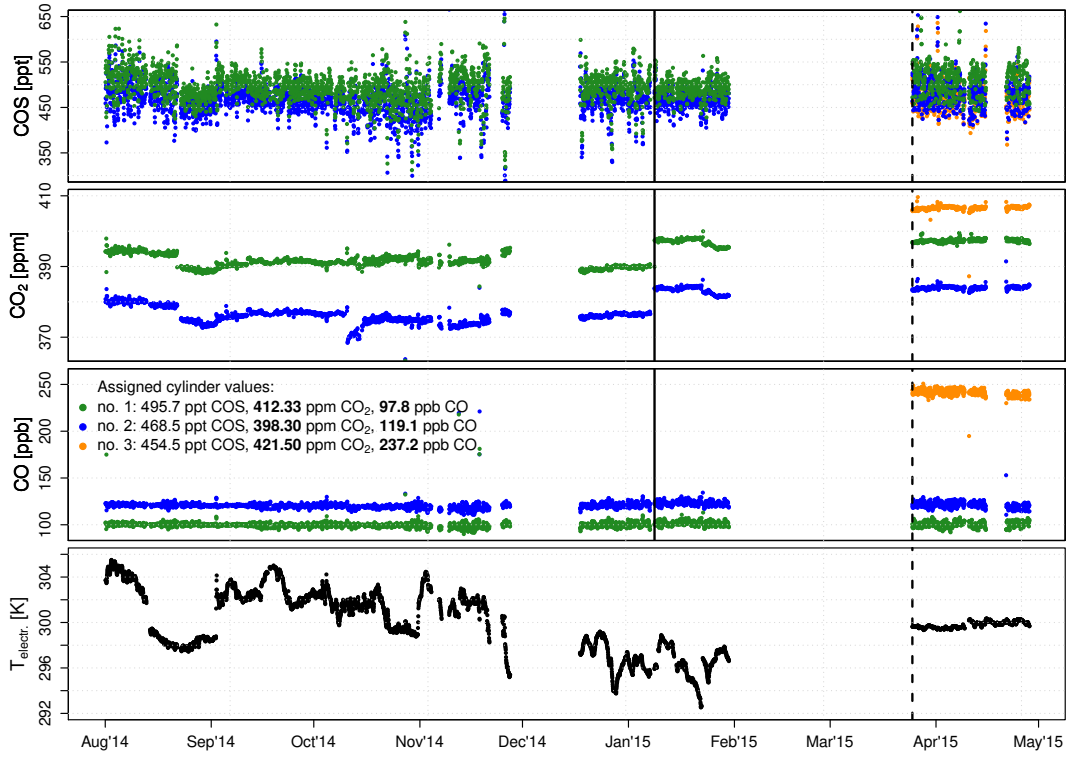

Figure 5. Mean concentrations of hourly measurements of working standards conducted while the instrument was in the field from August 2014 until April 2015 together with electronics temperature. The data shown here are uncorrected data and are not calibrated with a response curve. The concentrations are therefore not necessarily close to the assigned cylinder values. The solid vertical line at 7 January 2015 indicates the moment when we changed the setup with a solenoid valve to a Valco valve for switching to nitrogen, as the solenoid valve was leaking. The dashed vertical line at 25 March 2015 indicates the moment when we improved the temperature stability by actively cooling the electronics section and putting the analyzer in an enclosed box, which resulted in substantially smaller temperature fluctuations than before. From this moment onwards an extra working standard was also measured every hour to ascertain if the instrument response was stable over a period of 35 days (orange). The gap in the data record in December 2014 and February–March 2015 is because of tests with the QCLS in the laboratory.

ers the reference and target gases. In October 2014 the span between the two cylinder measurements changed, which is again mostly visible in CO_2. The reason for this change is that the regulator pressure of one of the two cylinders was slightly changed, which affected the amount of dilution of nitrogen into the sample line. Although it is known that COS mole fractions can drift in cylinders over time, we did not find indications that the mole fractions drifted within the measurement period. Later in this section we discuss the cylinder drift in more detail.

Figure 6 shows the 1-second standard deviations of the hourly reference gas measurements between August 2014 and April 2015. It is clear from Fig. 6 that the instrument precision cannot be captured with one single value due to its variation. For the period marked in red the room temperature was characterized by rapid changes caused by an air conditioner. This was a period in which the instrument precision was adversely affected, indicating that temperature stability influences the instrument precision. In the right plot of Fig. 6 the histograms of the standard deviations are shown for the periods before and after improvement of the temperature stability, with the black/gray colors corresponding to that in the left figure. The data show that for COS and CO_2 the period after improving the temperature stability has an improved mean standard deviation compared to the period before the temperature improvement (from 6.6 to 4.8 ppt for COS and from 0.14 to 0.06 ppm for CO_2). However, as there were also moments with better precision in August and September 2014, there is no consistent relation between temperature stability and instrument precision. What we do see is that the instrument precision changed every time that the mirror alignment was changed, indicated by blue vertical lines. During periods that the mirror alignment was not changed (January and April 2015), the instrument precision was stable. These results show that the instrument precision can largely be affected by the mirror alignment.

Allan deviation plots are an effective way to show how far the random noise level can be reduced by averaging and at what timescale the drift effect starts (Allan, 1987). However, we found that Allan deviation plots of the measure-

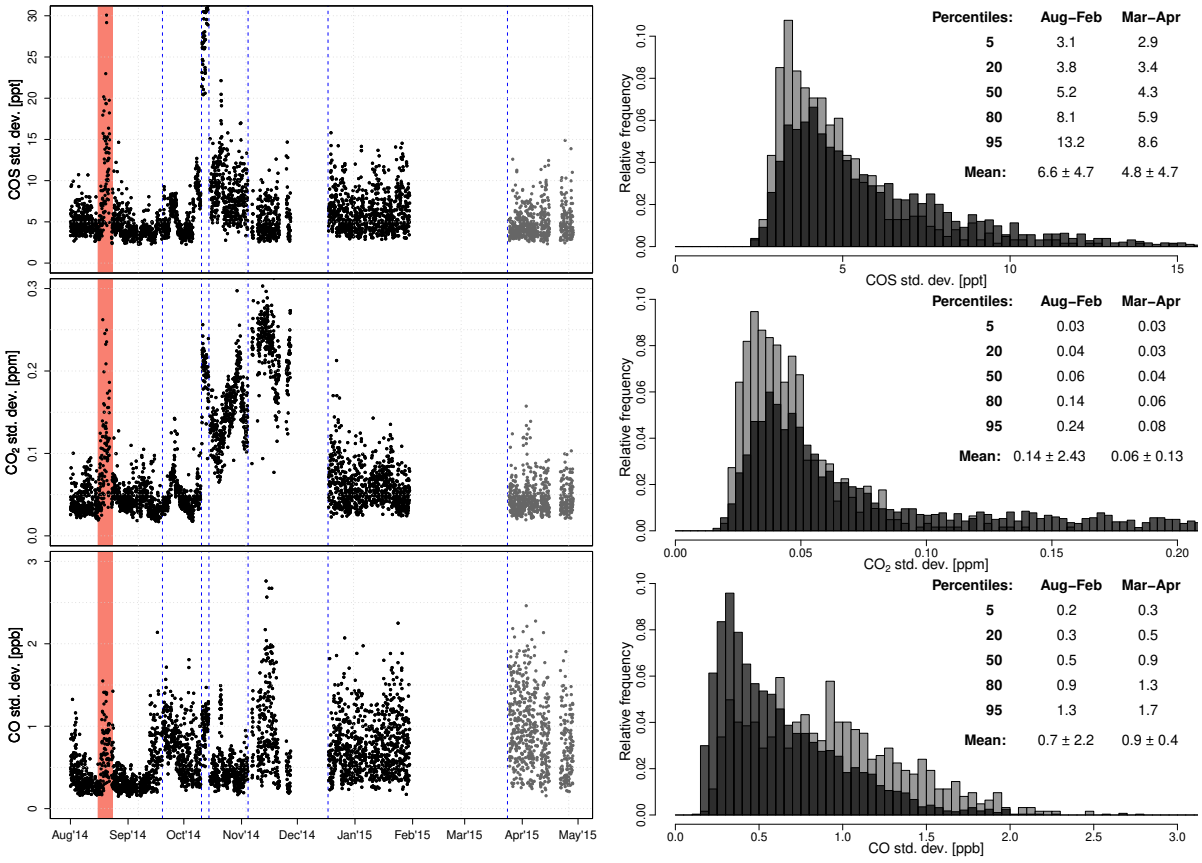

Figure 6. Left: standard deviation over 2 min of hourly measurements of one of the working standards as measured from August 2014 until April 2015. The gray (black) colored data indicate the period after (before) modifications were made to improve the temperature stability (such that T_{electr} varied with 0.21 °C with every degree of changing T_{room}, against 0.91 °C °C^{-1} before modifications; see Sect. 2.5). For the period that is marked with a red background the room temperature was characterized by rapid changes caused by an air conditioner. Blue vertical (dashed) lines indicate moments where the mirror alignment was changed. Right: histogram of standard deviations as shown in the left figure with the black/gray colors corresponding to the colors in the left figure. Note that the dark histogram is transparent. Also included are the mean standard deviations as well as an overview of percentiles because the data do not show a Gaussian distribution.

ments from the instrument is not consistent over time. As an example, we show two Allan deviation plots in Fig. 7. The data used in the two Allan deviation plots were retrieved from cylinder air measurements during two laboratory experiments under similar conditions on the same day. We find that the lowest random noise level of drift is not constant over time. The left Allan deviation plot in Fig. 7 shows that the noise level goes down to 0.6 ppt at 100 s, whereas in the right plot averaging does not lower the precision but rather increases it to 3.5 ppt at 100 s. The averaging time at which drift dominates Gaussian noise is around 2 s.

The overall uncertainty of the measurements consists of uncertainties associated with the scale transfer, water vapor corrections, drift correction and the measurement precision. Table 5 summarizes the different uncertainty contributions as well as the overall uncertainty for measurements of COS, CO_2 and CO. The overall uncertainty is calculated as the quadrature sum (square root of the sum of squares) of the individual uncertainties. The overall uncertainty that is presented in Table 5 characterizes the typical measurement uncertainty but may vary depending on the conditions. For example, the measurement precision varies, as we discussed in the previous paragraph, and the water vapor correction uncertainty scales with the COS, CO_2 and CO concentrations. In Table 5 we present 1-minute precisions that depend on the frequency of reference measurements (see Sect. 2.2.3 and Table 3). We adopted the 1-minute precision that is based on reference measurements made every 30 min, which represents the calibration strategy of our field measurements. Furthermore, precision depends on the length of the averaging period, where it can either decrease for Gaussian noise or increase for instrument drift. In Fig. 6 we can see that the 1-second precision of working standard measurements in March–April is 4.3 ppt for COS (50 % percentile of the measurements). The precision of 2-minute averaged target measurements in Fig. 8 (discussed later in this section) varies

Table 5. Uncertainty contributions and the overall uncertainty for measurements of COS (447.8–486.6 ppt), CO_2 (354–426 ppm) and CO (94–384 ppb), for the range of H_2O (0–2.1 %).

Uncertainty contributions	COS [ppt]	CO_2 [ppm]	CO [ppb]
Repeatability of the NOAA or WMO scale[a]	2.1	0.07	2.0
Transfer scale to working standards (1σ)[b]	2.8	0.12	1.7
Measurement calibration[c]	2.8	0.12	1.7
Water vapor correction (1σ)	2.9	0.10	1.1
Measurement precision (1 min)[d]	5.3	0.09	0.3
Overall uncertainty	7.5	0.23	3.3

[a] For COS: defined as the standard deviation of the measurements associated with the cylinder calibration. For CO_2 and CO: certified by the WMO central calibration laboratory (NOAA/ESRL).
[b] Average uncertainty over four cylinders in Table 2 (method 3).
[c] Using the single bias correction (see Sect. 2.2.2) it is the same as transferring the scale to the working standards.
[d] The standard deviation over minute-averaged cylinder measurements after drift correction with reference measurements every 30 min (Table 3).

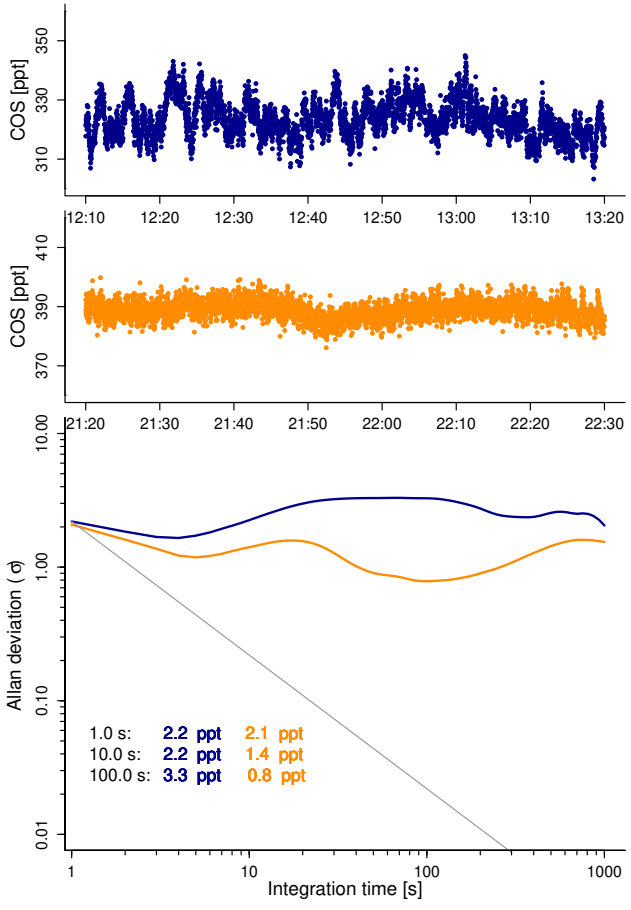

Figure 7. Two Allan deviation plots of COS retrieved from cylinder air measurements during two laboratory experiments under similar conditions on the same day. The Allan deviation plots show that the lowest random noise level of drift is not constant over time.

between 4.9 and 6.6 ppt. These numbers reflect the typically higher values for precision on longer timescales than 1 s due to instrument drift. We provide the numbers for COS here, but the same holds for CO_2 and CO.

We have now presented the total uncertainty for long-term concentration monitoring at an atmospheric station, but not all uncertainties are relevant for every type of analyses. If the data are to be compared across different sites, then the data should be on the same scale and the accuracy of the measurements is important. However, if data from the same site and the same instrumentation are compared, for example to do flux-gradient analysis, then there is a less stringent need for accuracy and the short-term precision is more important. If the uncertainties related to the transfer of the scales are not taken into account, then the total uncertainty would be 6.0 ppt for COS, 0.13 ppm for CO_2 and 1.1 ppb for CO. This includes both the uncertainty of the water vapor correction and the 1-minute measurement precision. The uncertainty of the water vapor correction cannot simply be ignored as gradients in H_2O can exist as well. We observed that COS concentrations between 40 and 7 m differ on average by 1.7 ± 5.3 ppt during daytime and 11.4 ± 33.0 ppt during nighttime. Given that the gradients should be larger than the uncertainties mentioned above, the daytime gradients are too small to be able to use the flux-gradient method. The suitability of the flux-gradient method is further dependent on the choice of the measurement height (gradients are larger closer to the surface), the size of the fluxes at a given site and the turbulence conditions. Even though the use of the flux-gradient method is limited by the measurement uncertainty that we found here, COS profile measurements from this instrument can still be useful to derive storage fluxes, as nighttime gradients are typically larger.

Additional to the uncertainties presented in Table 5, we have observed that COS can decrease over time in uncoated aluminum cylinders. First, we did not find indications that our working standards drifted during field measurements at the Lutjewad station; calibrations in July 2014 and March 2015 showed a decrease of only 2.2 and 1.1 ppt for cylinder nos. 1 and 2 over this 8-month period, which is well within

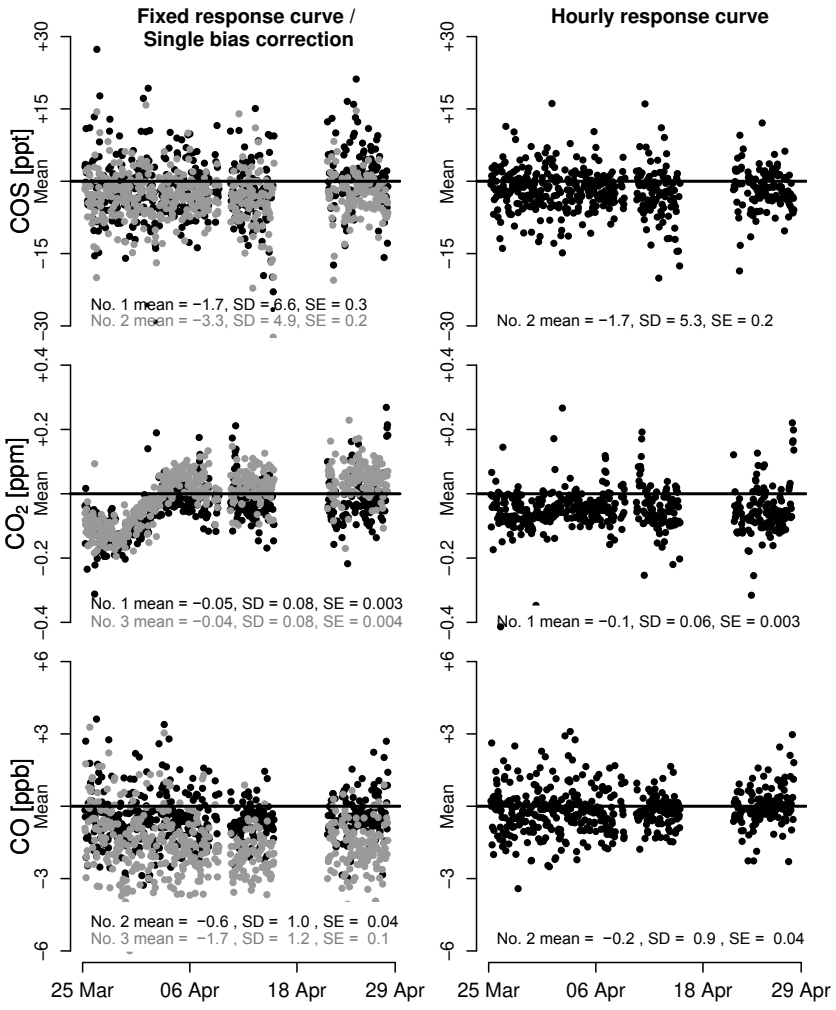

Figure 8. Mole fraction offsets in target standards after application of (left) corrections with a fixed response curve for CO_2 and CO that was determined in the laboratory (see Sect. 2.2.1) and with a single bias correction for COS, and (right) corrections with changing response curves determined from the hourly measurements of working standards. For the fixed response curve measurements of two target standards are shown, for the hourly response curve only one is shown, as two of the three working standards were needed to determine the response curve. The mean deviation from the assigned cylinder value, standard deviation (SD) and standard error (SE) are given for each target standard. The cylinder numbers (nos. 1, 2, 3) correspond with the cylinder numbers and assigned cylinders values given in Fig. 5.

the measurement uncertainty. However, a re-calibration in November 2015 showed a decrease of 18.2 and 24.1 ppt in these cylinders, a decrease with a rate of 2.3 and 3 ppt per month, while cylinder no. 3 only changed by 1.9 ppt. Cylinder no. 3 is not different from nos. 1 and 2 (they are all uncoated aluminum cylinders), but cylinder nos. 1 and 2 were stored with a pressure of 25 and 40 bar, which is lower than 130 bar for cylinder no. 3. We cannot confirm if the drift in the cylinders is related with the cylinder pressure; however, it is the only difference that we were able to find. Experience with cylinders over the past 15 years at NOAA indicates that COS in Aculife treated aluminum cylinders is typically much more stable than untreated aluminum cylinders. A potential method to improve COS calibrations is to calibrate these using a ppb-level standard accurately diluted to a range of desired COS concentrations (LaFranchi et al., 2015), provided the ppb-level standard is less susceptible to drifting COS concentrations. Applying this method could improve the accuracy of the calibration if the COS concentrations can be accurately and precisely provided over a broad range, thereby allowing for a more accurate determination of instrument response and a calibration curve. Besides that, this method will aid in assessing the stability of working standards.

Our COS measurements are reported on the NOAA-2004 scale and can be compared to the observations from the global network of NOAA/ESRL (e.g., Montzka et al., 2007). The same holds for CO_2 and CO on the WMO-X2007 CO_2 scale and WMO-X2004 CO scale. To test the accuracy of the measurements against the NOAA or WMO scale we analyzed the measurements of one/two target standards after

application of two corrections: (1) a correction factor as obtained from response curves of CO_2 and CO to transfer the data to the WMO scale and (2) a bias correction using a reference standard to remove instrument drift and to calibrate the data with the NOAA scale for COS. For measurements in March and April 2015 we determined hourly response curves from measurements of two working standards. For every species we took the standards with the outer concentration values such that the response curves span a wide concentration range. To analyze the need to determine hourly response curves, we corrected the data in two ways: (1) with a single bias correction for COS and a fixed response curve for CO_2 and CO, i.e., the one that we determined in the laboratory (see Fig. 2), shown in the left plots of Fig. 8; and (2) with changing response curves determined from the hourly working standard measurements, shown in the right plots of Fig. 8. For the fixed response curve, measurements of two target standards are shown; for the hourly response curve only one is shown, as two of the three working standards were needed to determine the response curve. After the corrections are applied, the mean offset of the measurements is within 3.3 ± 0.2 ppt for COS, 0.05 ± 0.003 ppm for CO_2 and 1.7 ± 0.1 ppb for CO over the period of 35 days. The standard errors indicate that the mean offset is significantly different from 0. Still, the offsets are within the expected uncertainty based on the relevant uncertainties listed in Table 5, namely the transfer to working standards and measurement calibration of which the quadrature sum is 4.0 ppt COS, 0.17 ppm CO_2 and 2.4 ppb CO. The instrument drift is significant, which is why the standard deviation of the series of 2-minute target measurements shown in Fig. 8 is higher than the standard error of a 2-minute target measurement, or even higher than the 1-second precision. The fact that the mean offsets are on the same order of magnitude as the expected uncertainties indicates that these uncertainties listed in Table 5 properly envelope the uncertainties of the field measurements. The slightly larger deviation from the CO assigned value for one of the two working standards with the fixed response correction is because this standard has a higher concentration than the reference standard (237.2 against 97.8 ppb) and therefore the uncertainty due to the bias correction is larger. The other target standard, which has a concentration of 119.1 ppb, is closer to the reference standard and only shows a deviation of -0.6 ppb. For CO_2 it is visible that using the fixed response curve gives a bias up to 0.2 ppm in the target measurements, which is not visible when using the hourly response curve. This bias is due to the fact that the response did change in the first 10 days of the period, after which it became stable. We could not relate the changing response curve to any parameter such as temperature or pressure. We did notice that the response curve was changing only in the period after the instrument was transported. A potential reason for the change could therefore be that the instrument still had to be stabilized after transportation. We did not find indications that the response curve for CO_2 changed outside the period between March and April. Except for the fact that the hourly response curve corrects for the changing response curve for CO_2, the changing response curve does not significantly remove scatter compared to the fixed response curve for CO_2 and CO; that is, the standard deviation of target measurements for the fixed response curve is not substantially lower when the hourly response curve was applied. Also, the target measurements are not consistently closer to the assigned values when the hourly response curve was applied. Furthermore, the fact that the use of hourly response curves does not give lower standard deviations for target measurements of COS compared to when the single bias correction is used indicates again that the response curves cannot accurately be determined for this species, which we discussed in Sect. 2.2.1 and 2.2.2 as well. As we have not seen indications that the response curve for CO_2 changes outside the period between March and April, we do not see the need to frequently determine the response curves with multiple standards. Moreover, if the response would change outside of the period in March and April as well, then the effect only reaches up to 0.2 ppm for CO_2. Taking into account logistical reasons (use of cylinder gases), we suggest correcting data with a single bias correction for COS and with a fixed response curve for CO_2 and CO as determined once with NOAA/ESRL calibration standards (see Sect. 2.2.1), together with a single bias correction from a reference standard.

3.2 Measurement comparison

In this section we make different measurement comparisons. First, we compare COS flask measurements using the QCLS with those analyzed with the GC-MS at NOAA/ESRL. Second, we compare QCLS in situ and flask measurements of COS in order to test if the water vapor correction that we determined in Sect. 2.3 sufficiently removes the effect of water vapor on calculated mole fractions. Third, we compare the in situ CO_2, CO and H_2O measurements from the QCLS with those of a collocated CRDS to assess the calibration strategy and water vapor correction presented in this study. Based on the previous sections, we applied the following corrections to the in situ QCLS data: (1) before 25 March 2015, the TDLWINTEL water vapor correction was applied with broadening coefficients 1.5 for COS and CO and 1.7 for CO_2. On top of this correction we applied a linear water correction curve for COS, CO_2 and CO as obtained with the TDLWINTEL correction turned on. After 25 March 2015, the TDLWINTEL correction was turned off and we applied the correction curve from Fig. 3 as obtained with the TDLWINTEL correction off. (2) The calibration correction curves as obtained in Sect. 2.2.1, Fig. 2, were applied to transfer the data to the WMO scales for CO_2 and CO. (3) A bias correction was applied to remove instrument drift and to calibrate the data with the NOAA scale for COS; here we used the same, and single, reference standard over the whole measurement period.

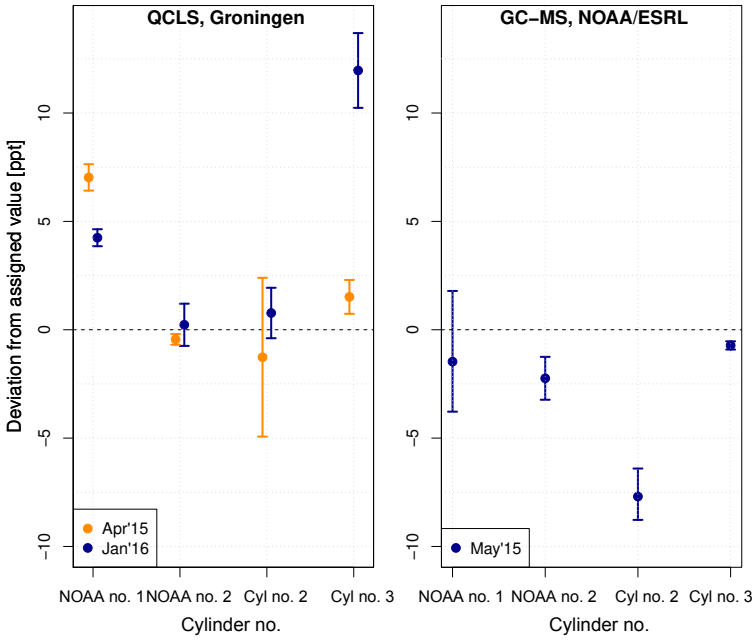

Figure 9. Flask sample measurements at the QCLS in Groningen (left) and GC-MS by NOAA/ESRL (right). Four paired flasks were filled with dry air from the two NOAA/ESRL calibration standards and two working standards, which were calibrated as in Sect. 2.2.2. The flask pair measurements are averaged and shown as the deviation from the assigned cylinder value. The first two cylinders are those calibrated at NOAA/ESRL and have an assigned value of 447.8 ppt (NOAA no. 1) and 486.6 ppt (NOAA no. 2). The last two cylinders were used as working standards in Lutjewad and have assigned values of 467.6 ppt (no. 3) and 455.5 ppt (no. 4). The error bars show the precision. For the QCLS two measurements were done: in April 2015 (orange) and in January 2016 (blue). The GC-MS measurement at NOAA/ESRL was performed in May 2015.

For the QCLS and GC-MS instrument comparison an overview of the measurements is given in Fig. 9, where the flask pair measurements are averaged and are shown as the deviation from the assigned cylinder value (see also Sect. 2.6). The precision within the flask pair is shown by the error bars. The comparison demonstrates the uncertainties associated with the transfer to the NOAA scale (see Table 5). For the first measurement at the QCLS (orange), three of the four flask pairs are within 1.5 ppt of the assigned value and one flask pair deviates by 7 ppt. This is similar to the GC-MS measurements at NOAA where one of the four flask pairs deviates further from the assigned values. However, the deviating flask pair measured by the GC-MS is not the same as the one deviating at the QCLS. For the second QCLS measurement (blue) one flask pair has drifted on average by 12 ppt, where other flasks remained stable within 2.5 ppt. It is unclear why the two flasks have drifted as all flasks were filled, measured and stored in the same way; however, we have kept the pair to monitor the potential drift in the future and to find out what has caused the drift. Moreover, the consistency of the flask measurements between April 2015 and January 2016 is dependent on the stability of the reference standard which was used for all flask measurements. Although we observed that COS can drift in cylinders, we did not find indications that the particular reference standard used for this analysis drifted over the 9-month period. The flask pairs have a mean deviation from the assigned cylinder values of +3.0 ppt for the QCLS (1.7 ppt when excluding the drifting flask pair) and −3.0 ppt for the GC-MS measurements. Although these deviations are within the QCLS measurement uncertainty of 6.9 ppt (including transfer of scales and the measurement precision), the GC-MS measurements are consistently lower than those from the QCLS, with an average difference of 5.1 ppt (excluding the drifting flask pair). We were not able to find an explanation for this bias.

The next comparison in Fig. 10 considers the in situ COS measurements between 25 March and 29 April 2015 and 11 dry air flask samples measured by the same QCLS. The flasks are flushed for an hour before closing, but because of mixing in the flask we assume that the flask sample represents the last 15 min; therefore we average the in situ measurements over these 15 min. The flask samples have an inlet at 60 m height, but because the in situ 60 m measurements only cover the period between 9 and 15 min before flask closure we also include 40 m measurements to cover the last 9 min before the flask is closed. The average difference of COS mole fractions between the 40 and 60 m level is 0.7 ± 9.7 ppt (40–60 m) over the measurement period in March and April. Although the mean difference of 0.7 ppt is not significant, the 9.7 ppt standard deviation points to actual differences between the 40

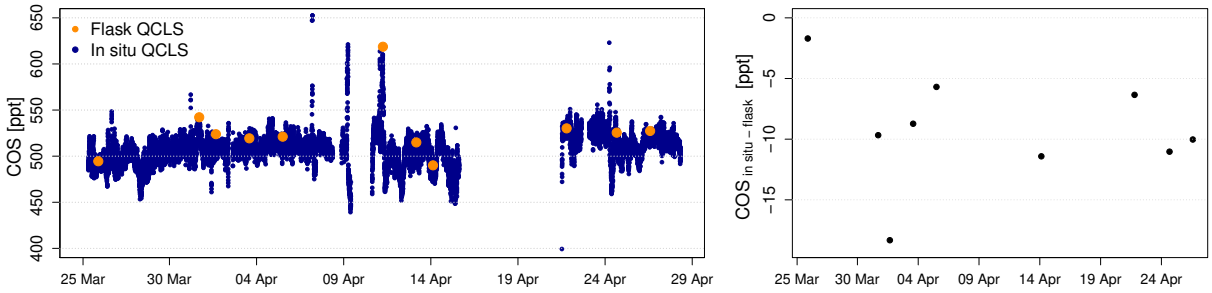

Figure 10. Minute-averaged measurements of COS at the Lutjewad measurement tower (60 m) between 25 March and 29 April 2015 as measured in situ by the QCLS (blue), compared with dry air flasks samples measured at the QCLS (orange). The left plots show the time series; the right plots show the difference between the in situ and flask measurement.

and 60 m concentrations. For the moments when the flask and in situ measurements are compared, the difference is -4.2 ± 3.4 ppt. We neglected one flask–in situ pair for which the 40 and 60 m difference was larger than 10 ppt. For the remaining data we do not expect a large bias associated with including ongoing results from the 40 m height in the averages. Peaks and valleys in COS mole fractions shown in Fig. 10 are well covered by both sampling techniques (flasks and in situ); for example, the peak up to 620 ppt at 11 April is clearly visible in both the in situ and flask measurements. The average difference between the in situ and flask measurements (in situ–flask) is -9.7 ± 4.6 ppt. Besides neglecting one flask measurement where the 40–60 m difference was larger than 10 ppt, we neglected one flask sample where the in situ COS measurement over 15 min showed large variation (standard deviation of 17.5 ppt where the average standard deviation of the other periods is only 4.7 ppt) and thereby introduced an error in the comparison. The average difference of -9.7 ppt could be caused by the uncertainty of the flask and the in situ measurements (where the latter includes the uncertainty of the water vapor correction), the sampling bias of both in situ and flask measurements, as well as the storage effect of air in the flasks. In Table 5 we quantified the uncertainty related to the transfer of the scale to working standards and measurements, the water correction and the measurement precision. The uncertainty related to the repeatability of the NOAA scale cancels out for the flask–in situ comparison. Combining these uncertainties gives an uncertainty of 6.6 ppt for the flasks and 7.2 ppt for the in situ measurements (with the uncertainty of the water vapor correction included). The combined uncertainty of both methods is 9.8 ppt, which is very similar to the -9.7 ppt difference that we found. We were not able to test the effect of biases resulting from the sampling of flasks. We find that after applying the water correction to the in situ data, the flask–in situ difference does not show a correlation with H_2O ($R^2 = 0.01$; slope = 3.9 ppt COS per % H_2O), whereas without water vapor correction there is a correlation with H_2O ($R^2 = 0.36$; slope = 26.3 ppt COS per % H_2O), which demonstrates that our laboratory-derived water vapor correction properly corrects for the effect of water vapor.

Last, we compare the minute-averaged QCLS measurements for CO_2, CO and H_2O with those made by a collocated CRDS in Fig. 11. The air samples were taken from the same height but through a different inlet. The CRDS measurements of CO_2 and CO were performed on humid air and were corrected for water vapor dilution and interference effects based on a set of instrument-specific correction factors determined in the laboratory of the Center for Isotope Research before field deployment (Chen et al., 2010, 2013). The comparison was only made from 7 January onwards because before that period there was the problem of nitrogen leaking into the sample air for which we used the CRDS data to correct for the dilution. There are no temporal patterns visible in the difference plot on the right of Fig. 11. The mean differences (QCLS−CRDS) are -0.12 ± 0.77 ppm for CO_2, -0.9 ± 3.8 ppb for CO and -0.01 ± 0.09 % for H_2O. For H_2O there were problems with water vapor in the sample lines in March and April, so we only calculated the difference for H_2O over the month January. A correlation of the CRDS and QCLS data of both CO_2 and CO (slope = 0.98) indicates that there is no concentration-dependent offset. Also, no correlation was found between water vapor and the difference between CRDS and the QCLS CO_2 and CO data (CO_2: slope = 0.16, $R^2 = 0.003$; CO: slope = 0.48, $R^2 = 1.9 \times 10^{-5}$). These results give confidence in the calibration strategy and water vapor correction presented in this study. For the period up to 29 January, the TDLWINTEL water vapor correction was turned on, and on top of this correction we applied the linear water correction curves as obtained with the TDLWINTEL correction turned on. If we would not apply this linear correction curve on top of the TDLWINTEL correction, then the median difference between the QCLS and CRDS measurements for this period would be -0.59 ppm for CO_2 and -1.1 ppb for CO (against -0.02 ppm and -0.9 ppb for specifically this period when the linear correction curve is applied).

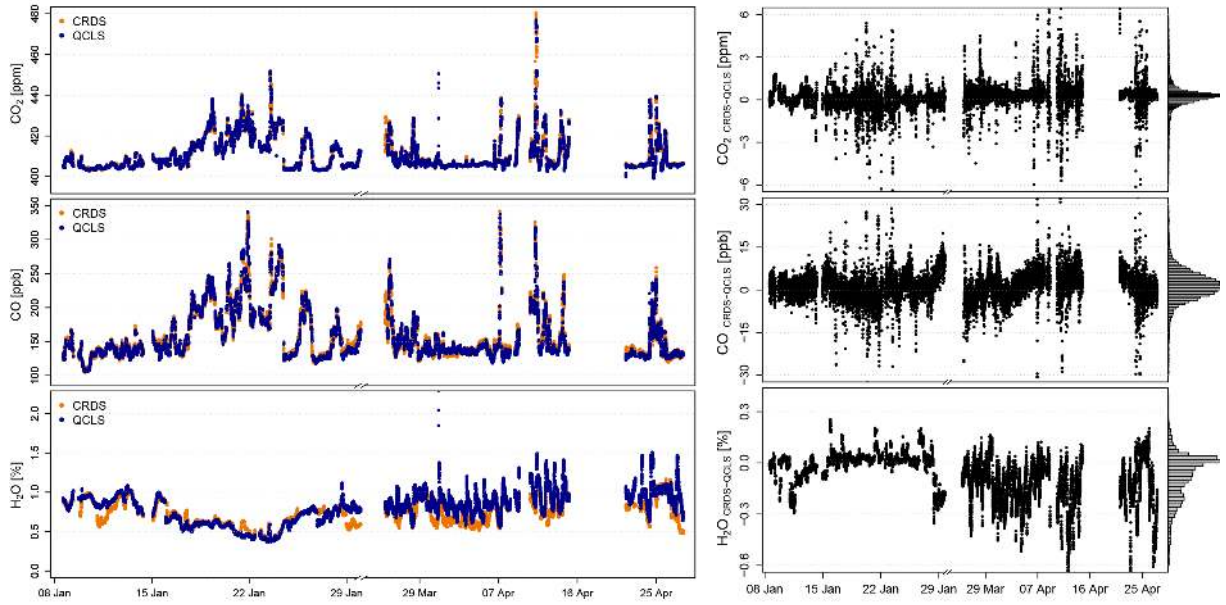

Figure 11. Minute-averaged measurements of CO_2, CO and H_2O from the Lutjewad measurement (60 m) tower between 7 January and 29 April 2015 as measured by the QCLS (blue), compared with measurements from a CRDS (orange). The left plots show the time series and the right plots show the difference between CRDS and QCLS measurements together with the frequency distribution of the difference, which is plotted as a histogram.

3.3 Continuous COS, CO_2, CO and H_2O observations from Lutjewad

The COS, CO_2, CO and H_2O data record obtained at the 60 m level of the Lutjewad tower is presented in Fig. 12. The data corrections used for these data were summarized in the previous section. Besides of these corrections we corrected for the dilution of nitrogen due to a leaking solenoid valve before 7 January 2015. We determined a dilution factor by comparing CO_2 measurements from the QCLS and a CRDS from the same location and height, under the assumption that without dilution the two analyzers measure the same concentrations (see Sect. 3.2). The percentage of dilution was calculated for CO_2 and was typically between 0.4 and 4.9 %. These dilution factors were then applied to all species.

The location of the Lutjewad station along the coast of the province of Groningen in the Netherlands allows the measurement of marine background air during northerly winds and continental air during southerly winds (van der Laan et al., 2009). Daytime CO_2 concentrations are typically correlated with elevated CO concentrations, indicating the influence of local and regional fossil fuel emissions (van der Laan et al., 2010). Even though the data do not cover a full year cycle, it can be seen that the seasonal amplitude of CO_2 mole fractions is approximately 15 ppm with a minimum around the end of August. The seasonal variation of CO_2 for the Lutjewad measurement station is analyzed in detail by van der Laan-Luijkx et al. (2010) and Van Leeuwen et al. (2015). The seasonal cycle of COS is captured well by the QCLS and the peak-to-peak amplitude is estimated to be 96 ppt based on the two-harmonic fit. Kettle et al. (2002) showed that vegetative uptake is the flux with the largest seasonal cycle on the NH, and Montzka et al. (2007) showed that the seasonal amplitude of COS depends on the degree to which the sampled air is influenced by terrestrial ecosystems. It is therefore likely that the seasonal variation of COS observed at the Lutjewad site is influenced by vegetative uptake. In Fig. 13 we compare COS mole fractions from Lutjewad with that from three other sites as measured from flask samples with a GC-MS by NOAA/ESRL Montzka et al. (2007). The flask samples cover data between 2000 and 2015 for Wisconsin, USA (LEF), and Mauna Loa, USA (MLO), and between 2001 and 2015 for Mace Head, Ireland (MHD). These data are an update of those presented in Montzka et al. (2007) (data available at ftp://ftp.cmdl.noaa.gov/hats/carbonyl_sulfide/). The flask measurements in Fig. 13 are plotted as function of time of the year. The high-altitude MLO site is less directly influenced by terrestrial ecosystems and therefore shows only small seasonal variation, in contrast to the LEF site, which is largely influenced by (forested) continental air. The Lutjewad COS mole fractions are most consistent with measurements from MHD, which can be expected since both stations are coastal sites and are located at similar latitudes. The seasonal amplitude of COS at MHD and Lutjewad is in between that of LEF and MLO, most likely because both sites are not solely influenced by marine or continental air but by both types of air masses. The COS mole fraction has a minimum in Septem-

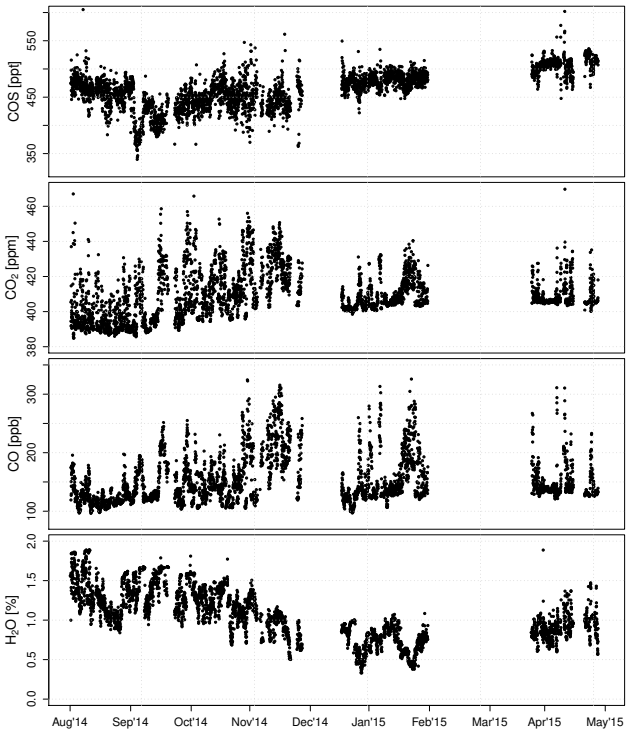

Figure 12. Hourly-averaged measurements of COS, CO_2, CO and H_2O in ambient air at the 60 m level of the Lutjewad measurement tower as measured by the QCLS. Data are shown with corrections as described in the text.

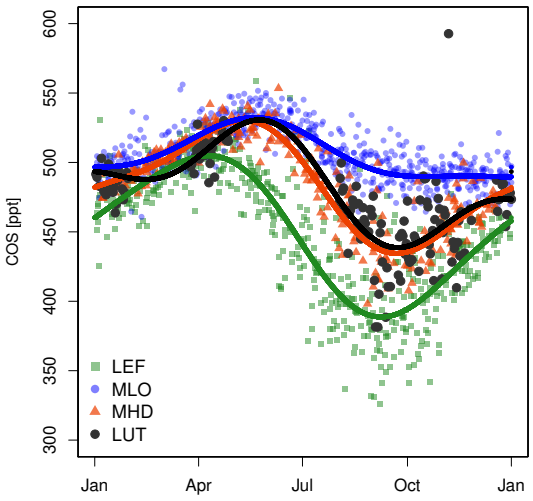

Figure 13. COS seasonal cycle of four sites: Wisconsin, USA (LEF); Mauna Loa, USA (MLO); Mace Head, Ireland (MHD); and Lutjewad, the Netherlands (LUT); the data of the latter site are presented in this study. COS mole fractions for the LEF, MLO and MHD sites were measured from flask samples at a GC-MS by NOAA/ESRL (Montzka et al., 2007). The NOAA/ESRL data are shown as flask pair means from individual sampling events. All NOAA measurements are plotted as function of time of the year and cover a period between 2000 and 2015 for LEF, MLO and MHD. In situ COS measurements with the QCLS at the Lutjewad site during 2014–2015 are shown as daily averages (black). A two-harmonic seasonal cycle is fit through the data.

ber and October and is a few weeks later than the minimum of the CO_2 mole fraction. Montzka et al. (2007) and Blonquist et al. (2011) also observed a COS minimum later than that of CO_2. They reasoned that this difference is due to the fact that at the end of the growing season COS mole fractions keep decreasing due to vegetative uptake without at the same time having a source of COS, whereas during this time of year respiration is beginning to offset assimilation in determining the ambient CO_2 mole fractions.

4 Conclusions

In this study we have tested a QCLS for its suitability for making accurate and high-precision measurements of COS, CO_2, CO and H_2O. First, the instrument response was characterized using calibration standards and to transfer raw data to the NOAA or WMO scale. Unfortunately, the range of mole fractions in the calibration standards did not allow the COS response to be accurately determined over the entire range of measured mole fractions. Based on an analysis of different calibration methods, however, we concluded that the measurements and working standards were best calibrated using a single bias correction for COS. From hourly paired measurements of working standards we observed changes in the response curve for CO_2 over a period of 10 days after transporting the instrument to the measurement site. However, as we have not seen indications that the response curve for CO_2 changed outside this period, and also taking into account logistical reasons (use of cylinder gases), we suggest calibrating field data with a fixed response curve for CO_2 and CO as determined once with calibration standards. Second, we investigated the needed frequency of background and reference measurements. Based on laboratory tests we have shown that background measurements every 6 h with reference measurements every 30 min (for removal of instrument drift) are sufficient to keep the standard deviation of working standard measurements within 5.3 ppt for COS, 0.09 ppm for CO_2 and 0.3 ppb for CO over a period of 19 h. We characterized the water vapor dependence of COS, CO_2 and CO from laboratory experiments. Based on an assessment of the TDLWINTEL water correction we determined optimal broadening coefficients for the use of the water correction within TDLWINTEL. Besides that, we presented an alternative water correction based on linear dependence of the wet air mole fractions with H_2O concentration. Furthermore, we demonstrate that a small H_2O peak close to the COS peak has caused a water-vapor-dependent concentration error that is larger than the direct water vapor dilution effect. This water vapor interference can be minimized by careful adjustments to the software fitting parameters and

was virtually eliminated with corrections as demonstrated in Fig. 3.

The QCLS was set up for continuous in situ measurements at different heights at the tower of the Lutjewad monitoring station. Hourly target measurements were used to assess the accuracy and precision of the measurements. After application of a calibration response curve for CO_2 and CO, and a single bias correction for removal of instrument drift and to calibrate the COS measurements to the NOAA scale, the target measurements showed a mean difference with the assigned cylinder value within 3.3 ppt for COS, 0.05 ppm for CO_2 and 1.7 ppb for CO over a period of 35 days. One-second precisions during reference gas flow were typically 4.3 ppt for COS, 0.04 ppm for CO_2 and 0.9 ppb for CO, but substantial variations in the instrument precision were observed during the 7-month field campaign. We improved the temperature stability of the QCLS by applying an additional insulation layer that is controlled by the same thermoelectric chiller as the one used for cooling the laser and detector. However, improvement of the temperature stability of the instrument did not show a consistent relation with instrument precision. We showed that variations in the precision were largely driven by mirror alignment. The different uncertainty contributions for measurements of COS, CO_2 and CO were summarized and the overall uncertainty was determined to be 7.5 ppt for COS, 0.23 ppm for CO_2 and 3.3 ppb for CO. We discussed the relevance of different uncertainty contributions for different types of analyses (e.g., differences across sites and interpreting profile measurements). Our setup with the QCLS provides sufficient accuracy and precision to detect gradients larger than 6.0 ppt for COS, 0.13 ppm for CO_2 and 1.1 ppb for CO. For the current setup in Lutjewad, the daytime gradients were too small compared to the measurement uncertainty to be able to use the flux-gradient method. QCLS measurements were compared with independent CRDS measurements for CO_2 and CO and with dry air flask samples at the QCLS for COS, which showed a mean difference of -9.7 ± 4.6 ppt for COS, 0.12 ± 0.77 ppm for CO_2, -0.9 ± 3.8 ppb for CO and -0.01 ± 0.09 % for H_2O. After correction for water vapor there was no correlation between the offsets and water vapor for all species. The measurement record over the 7-month period was presented and compared with NOAA/ESRL flask measurements for COS at other sites in the NH. The peak-to-peak amplitude of COS in ambient air at the Lutjewad monitoring station was estimated to be 97 ppt, which is comparable to other coastal sites at similar latitudes in the NH.

5 Data availability

The following data are available as a Supplement to this paper:

1. water vapor experiment data used in Fig. 3
2. time series of COS used for the Allan deviation plots in Fig. 7.

Other data from laboratory tests are available upon request (huilin.chen@rug.nl).

The flask measurements made by NOAA/ESRL as part of a COS monitoring network (Montzka et al., 2007) are available at ftp://ftp.cmdl.noaa.gov/hats/carbonyl_sulfide/.

The Supplement related to this article is available online at doi:10.5194/amt-9-5293-2016-supplement.

Acknowledgements. We would like to thank B. A. M. Kers, M. de Vries, H. G. Jansen and H. A. Been for their help in preparing the system for installation in the field and for maintenance of the instrumentation in Lutjewad. We thank D. Paul for the valuable discussions and suggestions, H. A. Scheeren for providing the CO_2 and CO calibrations of our working standards and J. J. Spriensma for her help in sorting out flask samples. We also acknowledge the preparation of gravimetric standards and working standards at NOAA by B. Hall and the technical assistance of C. Siso. Finally, we would like to thank the reviewers for their valuable comments and suggestions. This work was supported by the Dutch Sector Plan Physics.

Edited by: M. von Hobe
Reviewed by: two anonymous referees

References

Allan, D. W.: Time and Frequency (Time-Domain) Characterization, Estimation, and Prediction of Precision Clocks and Oscillators, IEEE T. Ultrason. Ferr., 34, 647–654, 1987.

Asaf, D., Rotenberg, E., Tatarinov, F., Dicken, U., Montzka, S. A., and Yakir, D.: Ecosystem photosynthesis inferred from measurements of carbonyl sulphide flux, Nat. Geosci., 6, 186–190, doi:10.1038/ngeo1730, 2013.

Belviso, S., Schmidt, M., Yver, C., Ramonet, M., Gros, V., and Launois, T.: Strong similarities between night-time deposition velocities of carbonyl sulphide and molecular hydrogen inferred from semi-continuous atmospheric observations in Gif-sur-Yvette, Paris region, Tellus B, 65, 20719, doi:10.3402/tellusb.v65i0.20719, 2013.

Berkelhammer, M., Asaf, D., Still, C., Montzka, S., Noone, D., Gupta, M., Provencal, R., Chen, H., and Yakir, D.: Constraining surface carbon fluxes using in situ measurements of carbonyl sulfide and carbon dioxide, Global Biogeochem. Cy., 28, 161–179, doi:10.1002/2013GB004644, 2014.

Berry, J., Wolf, A., Campbell, J. E., Baker, I., Blake, N., Blake, D., Denning, A. S., Kawa, S. R., Montzka, S. A., Seibt, U., Stimler, K., Yakir, D., and Zhu, Z.: A coupled model of the global cycles of carbonyl sulfide and CO_2: A possible new window on the carbon cycle, J. Geophys. Res.-Biogeo., 118, 842–852, doi:10.1002/jgrg.20068, 2013.

Blonquist, J. M., Montzka, S. A., Munger, J. W., Yakir, D., Desai, A. R., Dragoni, D., Griffis, T. J., Monson, R. K., Scott, R. L., and Bowling, D. R.: The potential of carbonyl sulfide as a proxy for gross primary production at flux tower sites, J. Geophys. Res.-Biogeo., 116, G04019, doi:10.1029/2011JG001723, 2011.

Campbell, J. E., Carmichael, G. R., Chai, T., Mena-Carrasco, M., Tang, Y., Blake, D. R., Blake, N. J., Vay, S. A., Collatz, G. J., Baker, I., Berry, J. A., Montzka, S. A., Sweeney, C., Schnoor, J. L., and Stanier, C. O.: Photosynthetic Control of Atmospheric Carbonyl Sulfide During the Growing Season, Science, 322, 1085–1088, doi:10.1126/science.1164015, 2008.

Chen, H., Winderlich, J., Gerbig, C., Hoefer, A., Rella, C. W., Crosson, E. R., Van Pelt, A. D., Steinbach, J., Kolle, O., Beck, V., Daube, B. C., Gottlieb, E. W., Chow, V. Y., Santoni, G. W., and Wofsy, S. C.: High-accuracy continuous airborne measurements of greenhouse gases (CO_2 and CH_4) using the cavity ring-down spectroscopy (CRDS) technique, Atmos. Meas. Tech., 3, 375–386, doi:10.5194/amt-3-375-2010, 2010.

Chen, H., Karion, A., Rella, C. W., Winderlich, J., Gerbig, C., Filges, A., Newberger, T., Sweeney, C., and Tans, P. P.: Accurate measurements of carbon monoxide in humid air using the cavity ring-down spectroscopy (CRDS) technique, Atmos. Meas. Tech., 6, 1031–1040, doi:10.5194/amt-6-1031-2013, 2013.

Commane, R., Herndon, S. C., Zahniser, M. S., Lerner, B. M., McManus, J. B., Munger, J. W., Nelson, D. D., and Wofsy, S. C.: Carbonyl sulfide in the planetary boundary layer: Coastal and continental influences, J. Geophys. Res.-Atmos., 118, 8001–8009, doi:10.1002/jgrd.50581, 2013.

Commane, R., Meredith, L. K., Baker, I. T., Berry, J. A., Munger, J. W., Montzka, S. A., Templer, P. H., Juice, S. M., Zahniser, M. S., and Wofsy, S. C.: Seasonal fluxes of carbonyl sulfide in a midlatitude forest, P. Natl. Acad. Sci. USA, 112, 14162–14167, doi:10.1073/pnas.1504131112, 2015.

LaFranchi, B., Bambha, R., Schrader, P., and Michelsen, H.: Characterization of continuous OCS, CO and CO_2 measurements at a tower site in Livermore, CA USA, 18th WMO/IAEA Meeting on Carbon Dioxide, Other Greenhouse Gases, and Related Measurement Techniques (GGMT), La Jolla, 13–17 September 2015, A10, 2015.

Kettle, A., Kuhn, U., von Hobe, M., Kesselmeier, J., and Andreae, M.: Global budget of atmospheric carbonyl sulfide: Temporal and spatial variations of the dominant sources and sinks, J. Geophys. Res.-Atmos., 107, 4658, doi:10.1029/2002JD002187, 2002.

Maseyk, K., Berry, J. A., Billesbach, D., Campbell, J. E., Torn, M. S., Zahniser, M., and Seibt, U.: Sources and sinks of carbonyl sulfide in an agricultural field in the Southern Great Plains, P. Natl. Acad. Sci. USA, 112, 14162–14167, doi:10.1073/pnas.1319132111, 2014.

McManus, J. B., Zahniser, M. S., Nelson, D. D., Jr., Shorter, J. H., Herndon, S., Wood, E., and Wehr, R.: Application of quantum cascade lasers to high-precision atmospheric trace gas measurements, Opt. Eng., 49, 111124, doi:10.1117/1.3498782, 2010.

Meredith, L. K., Commane, R., Munger, J. W., Dunn, A., Tang, J., Wofsy, S. C., and Prinn, R. G.: Ecosystem fluxes of hydrogen: a comparison of flux-gradient methods, Atmos. Meas. Tech., 7, 2787–2805, doi:10.5194/amt-7-2787-2014, 2014.

Miller, B. R., Weiss, R. F., Salameh, P. K., Tanhua, T., Greally, B. R., Mühle, J., and Simmonds, P. G.: Medusa: A Sample Preconcentration and GC/MS Detector System for in Situ Measurements of Atmospheric Trace Halocarbons, Hydrocarbons, and Sulfur Compounds, Anal. Chem., 80, 1536–1545, doi:10.1021/ac702084k, 2008.

Montzka, S., Aydin, M., Battle, M., Butler, J., Saltzman, E., Hall, B., Clarke, A., Mondeel, D., and Elkins, J.: A 350-year atmospheric history for carbonyl sulfide inferred from Antarctic firn air and air trapped in ice, J. Geophys. Res.-Atmos., 109, D22302, doi:10.1029/2004JD004686, 2004.

Montzka, S. A., Calvert, P., Hall, B. D., Elkins, J. W., Conway, T. J., Tans, P. P., and Sweeney, C.: On the global distribution, seasonality, and budget of atmospheric carbonyl sulfide (COS) and some similarities to CO_2, J. Geophys. Res.-Atmos., 112, D09302, doi:10.1029/2006JD007665, 2007.

Nelson, D. D., McManus, B., Urbanski, S., Herndon, S., and Zahniser, M.: High precision measurements of atmospheric nitrous oxide and methane using thermoelectrically cooled mid-infrared quantum cascade lasers and detectors, Spectrochim. Acta. A., 60, 3325–3335, doi:10.1016/j.saa.2004.01.033, 2004.

Neubert, R. E. M., Spijkervet, L. L., Schut, J. K., Been, H. A., and Meijer, H. A. J.: A Computer-Controlled Continuous Air Drying and Flask Sampling System, J. Atmos. Ocean. Tech., 21, 651–659, doi:10.1175/1520-0426(2004)021<0651:ACCADA>2.0.CO;2, 2004.

Novelli, P. C., Masarie, K. A., Lang, P. M., Hall, B. D., Myers, R. C., and Elkins, J. W.: Reanalysis of tropospheric CO trends: Effects of the 1997–1998 wildfires, J. Geophys. Res.-Atmos., 108, 4464, doi:10.1029/2002JD003031, 2003.

Protoschill-Krebs, G. and Kesselmeier, J.: Enzymatic Pathways for the Consumption of Carbonyl Sulphide (COS) by Higher Plants*, Bot. Acta, 105, 206–212, doi:10.1111/j.1438-8677.1992.tb00288.x, 1992.

Protoschill-Krebs, G., Wilhelm, C., and Kesselmeier, J.: Consumption of carbonyl sulphide (COS) by higher plant carbonic anhydrase (CA), Atmos. Environ., 30, 3151–3156, doi:10.1016/1352-2310(96)00026-X, 1996.

Rella, C. W., Chen, H., Andrews, A. E., Filges, A., Gerbig, C., Hatakka, J., Karion, A., Miles, N. L., Richardson, S. J., Steinbacher, M., Sweeney, C., Wastine, B., and Zellweger, C.: High accuracy measurements of dry mole fractions of carbon dioxide and methane in humid air, Atmos. Meas. Tech., 6, 837–860, doi:10.5194/amt-6-837-2013, 2013.

Rothman, L. S., Gordon, I. E., Babikov, Y., Barbe, A., Chris Benner, D., Bernath, P. F., Birk, M., Bizzocchi, L., Boudon, V., Brown, L. R., Campargue, A., Chance, K., Cohen, E. A., Coudert, L. H., Devi, V. M., Drouin, B. J., Fayt, A., Flaud, J.-M., Gamache, R. R., Harrison, J. J., Hartmann, J.-M., Hill, C., Hodges, J. T., Jacquemart, D., Jolly, A., Lamouroux, J., Le Roy, R. J., Li, G., Long, D. A., Lyulin, O. M., Mackie, C. J., Massie, S. T., Mikhailenko, S., Müller, H. S. P., Naumenko, O. V., Nikitin, A. V., Orphal, J., Perevalov, V., Perrin, A., Polovtseva, E. R., Richard, C., Smith, M. A. H., Starikova, E., Sung, K., Tashkun, S., Tennyson, J., Toon, G. C., Tyuterev, V. G., and Wagner, G.: The HITRAN2012 molecular spectroscopic database, J. Quant. Spectrosc. Ra., 130, 4–50, doi:10.1016/j.jqsrt.2013.07.002, 2013.

Sandoval-Soto, L., Stanimirov, M., von Hobe, M., Schmitt, V., Valdes, J., Wild, A., and Kesselmeier, J.: Global uptake of carbonyl sulfide (COS) by terrestrial vegetation: Estimates corrected

by deposition velocities normalized to the uptake of carbon dioxide (CO_2), Biogeosciences, 2, 125–132, doi:10.5194/bg-2-125-2005, 2005.

Santoni, G. W., Lee, B. H., Goodrich, J. P., Varner, R. K., Crill, P. M., McManus, J. B., Nelson, D. D., Zahniser, M. S., and Wofsy, S. C.: Mass fluxes and isofluxes of methane (CH_4) at a New Hampshire fen measured by a continuous wave quantum cascade laser spectrometer, J. Geophys. Res.-Atmos., 117, D10301, doi:10.1029/2011JD016960, 2012.

Seibt, U., Kesselmeier, J., Sandoval-Soto, L., Kuhn, U., and Berry, J. A.: A kinetic analysis of leaf uptake of COS and its relation to transpiration, photosynthesis and carbon isotope fractionation, Biogeosciences, 7, 333–341, doi:10.5194/bg-7-333-2010, 2010.

Stimler, K., Nelson, D., and Yakir, D.: High precision measurements of atmospheric concentrations and plant exchange rates of carbonyl sulfide using mid-IR quantum cascade laser, Glob. Change Biol., 16, 2496–2503, doi:10.1111/j.1365-2486.2009.02088.x, 2010a.

Stimler, K., Montzka, S. A., Berry, J. A., Rudich, Y., and Yakir, D.: Relationships between carbonyl sulfide (COS) and CO_2 during leaf gas exchange, New Phytol., 186, 869–878, doi:10.1111/j.1469-8137.2010.03218.x, 2010b.

van der Laan, S., Neubert, R. E. M., and Meijer, H. A. J.: Methane and nitrous oxide emissions in The Netherlands: ambient measurements support the national inventories, Atmos. Chem. Phys., 9, 9369–9379, doi:10.5194/acp-9-9369-2009, 2009.

van der Laan, S., Karstens, U., Neubert, R. E. M., Van der Laan-Luijkx, I. T., and Meijer, H. A. J.: Observation-based estimates of fossil fuel-derived CO_2 emissions in the Netherlands using Delta 14C, CO and 222Radon, Tellus B, 62, 389–402, doi:10.1111/j.1600-0889.2010.00493.x, 2010.

van der Laan-Luijkx, I. T., Neubert, R. E. M., van der Laan, S., and Meijer, H. A. J.: Continuous measurements of atmospheric oxygen and carbon dioxide on a North Sea gas platform, Atmos. Meas. Tech., 3, 113–125, doi:10.5194/amt-3-113-2010, 2010.

Van Leeuwen, C.: Highly precise atmospheric oxygen measurements as a tool to detect leaks of carbon dioxide from Carbon Capture and Storage sites, PhD thesis, University of Groningen, the Netherlands, 2015.

White, M. L., Zhou, Y., Russo, R. S., Mao, H., Talbot, R., Varner, R. K., and Sive, B. C.: Carbonyl sulfide exchange in a temperate loblolly pine forest grown under ambient and elevated CO_2, Atmos. Chem. Phys., 10, 547–561, doi:10.5194/acp-10-547-2010, 2010.

Wohlfahrt, G., Brilli, F., Hoertnagl, L., Xu, X., Bingemer, H., Hansel, A., and Loreto, F.: Carbonyl sulfide (COS) as a tracer for canopy photosynthesis, transpiration and stomatal conductance: potential and limitations, Plant Cell Environ., 35, 657–667, doi:10.1111/j.1365-3040.2011.02451.x, 2012.

Xiang, B., Nelson, D. D., McManus, J. B., Zahniser, M. S., Wehr, R. A., and Wofsy, S. C.: Development and field testing of a rapid and ultra-stable atmospheric carbon dioxide spectrometer, Atmos. Meas. Tech., 7, 4445–4453, doi:10.5194/amt-7-4445-2014, 2014.

Zhao, C. L. and Tans, P. P.: Estimating uncertainty of the WMO mole fraction scale for carbon dioxide in air, J. Geophys. Res.-Atmos., 111, D08S09, doi:10.1029/2005JD006003, 2006.

Zhao, F. and Zeng, N.: Continued increase in atmospheric CO_2 seasonal amplitude in the 21st century projected by the CMIP5 Earth system models, Earth Syst. Dynam., 5, 423–439, doi:10.5194/esd-5-423-2014, 2014.